

Review

Binders for Li-Ion Battery Technologies and Beyond: A Comprehensive Review

Muskan Srivastava , Anil Kumar M. R. and Karim Zaghib * 

Department of Chemical and Materials Engineering, Concordia University, 1455 De Maisonneuve Blvd. West, Montreal, QC H3G 1M8, Canada; mu_sriva@live.concordia.ca (M.S.); anil.mr@concordia.ca (A.K.M.R.)

* Correspondence: karim.zaghib@concordia.ca

Abstract: The effects of global warming highlight the urgent need for effective solutions to this problem. The electrification of society, which occurs through the widespread adoption of electric vehicles (EVs), is a critical strategy to combat climate change. Lithium-ion batteries (LIBs) are vital components of the global energy-storage market for EVs, and sodium-ion batteries (SIBs) have gained renewed interest owing to their potential for rapid growth. Improved safety and stability have also put solid-state batteries (SSBs) on the chart of top batteries in the world. This review examines three critical battery technologies: LIBs, SIBs, and SSBs. Although research has historically concentrated on heavier battery components, such as electrodes, to achieve high gravimetric density, binders, which comprise less than 5% of the battery weight, have demonstrated great promise for meeting the increasing need for energy storage. This review thoroughly examines various binders, focusing on their solubilities in water and organic solvents. Understanding binder mechanisms is crucial for developing binders that maintain strong adhesion to electrodes, even during volume fluctuations caused by lithiation and delithiation. Therefore, we investigated the different mechanisms associated with binders. This review also discusses failure mechanisms and innovative design strategies to improve the performance of binders, such as composite, conductive, and self-healing binders. By investigating these fields, we hope to develop energy storage technologies that are more dependable and efficient while also helping to satisfy future energy needs.



Citation: Srivastava, M.; M. R., A.K.; Zaghib, K. Binders for Li-Ion Battery Technologies and Beyond: A Comprehensive Review. *Batteries* **2024**, *10*, 268. <https://doi.org/10.3390/batteries10080268>

Academic Editor: Seiji Kumagai

Received: 10 June 2024

Revised: 16 July 2024

Accepted: 19 July 2024

Published: 26 July 2024



Copyright: © 2024 by the authors. Licensee MDPI, Basel, Switzerland. This article is an open access article distributed under the terms and conditions of the Creative Commons Attribution (CC BY) license (<https://creativecommons.org/licenses/by/4.0/>).

Keywords: lithium-ion batteries; sodium-ion batteries; solid-state batteries; binders; failure mechanism; design strategies

1. Introduction

The impact of global warming on climate change has attracted societal attention to renewable energy sources (RESs). Failure to reduce the level of greenhouse gas (GHG) emissions in the atmosphere in the coming years increases the risk that global temperatures will exceed the threshold of 1.5 °C established by the International Panel on Climate Change (IPCC) in October 2018 [1,2]. The global CO₂ concentration in the atmosphere reached 417.1 ppm in 2022, an increase of 23% compared to that recorded in 1980 [3]. The primary factor responsible for GHG emissions is the burning of fuels to produce electricity. The increase in these emissions has heightened the necessity for breakthroughs in energy technologies to fulfill the expanding requirements of society beyond the limitations of fossil fuels.

Several new policies have been implemented to address rising global temperatures during the November 2023 Conference of the Parties (COP 28). One key strategy is the Global Renewables and Energy Efficiency Pledge. The USD 5 billion in funding granted to this pledge aims to assist 132 countries in advancing RESs and enhancing their efficiency by 2030 [4]. In addition to other technological developments, this pledge highlighted the significance of electrification. Electrical vehicles (EVs) are critical tools for electrifying society and can substantially reduce CO₂ emissions from transportation vehicles, which

account for 14% of the world's GHG emissions [5]. According to the International Energy Agency (IEA), to achieve the goal of net-zero emissions by 2050, a 3% annual reduction in CO₂ emissions is necessary until 2030 [6].

EVs are good alternatives to vehicles with internal combustion engines because of their reduced dependency on oil and zero emissions [7]. The IEA projects a cumulative total sale of nearly 45 million EVs by 2030, as indicated in Figure 1 [8]. Various EV policies, such as the United States Inflation Reduction Act (IRA), the European Union Green Deal Industry Plan, and India's Production-Linked Incentives, have been implemented to encourage the use of EVs [9]. With the surge in the use and development of EVs, the demand for high gravimetric energy density, high volumetric energy density, long cyclability, enhanced stability and safety, and low-cost rechargeable batteries has also increased [10–12]. High-capacity commercialized batteries are needed not only for EVs but also for storing other RESs, such as wind and solar. The market is currently flooded with various kinds of batteries, where the most popular ones include lithium-ion batteries (LIBs), solid-state batteries (SSBs), nickel-metal hydride (NMH), and some metal-ion batteries, such as sodium-ion batteries (SIBs), Zn-ion, Al-ion, and Mg-ion batteries [13–15]. This study focused on three main technologies: LIBs, SSBs, and SIBs. LIBs have paved the way for digital evolution and are present everywhere in our everyday lives, from cellphones and laptops to EVs [16,17]. In addition, given current technological advancements, SIBs have revived their position in the market. Their popularity is attributed to their low cost and superior safety [18]. Among battery scientists, the term "solid-state battery" has gained a lot of interest because these batteries have the potential to outperform LIBs in terms of both energy density and safety [19].

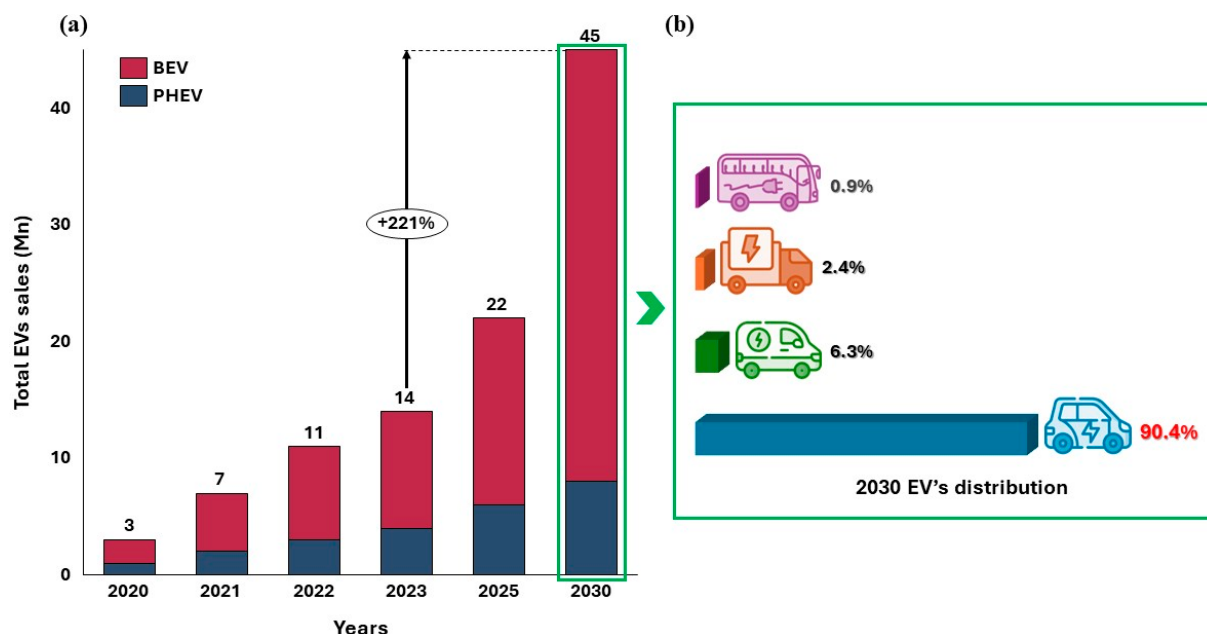


Figure 1. (a) Projected global EVs sales till the year 2030 for the region “world” using the Global EV Data Explorer tool [8]. (b) The distribution of total EV sales in 2030 is categorized by vehicle type as follows: buses (0.9%), trucks (2.4%), vans (6.3%), and cars (90.4%).

Batteries consist of various components, such as electrodes, electrolytes, and current collectors. Most of the battery weight consists of these components, with binders and additives contributing far less to the overall weight [20]. Since the invention of rechargeable battery technology, research and development efforts have mostly focused on electrode materials and electrolytes [21–26]. Although binders are a critical component of batteries, they are typically ignored by battery engineers [11,27]. However, the rising demand for high-energy-density rechargeable batteries has focused attention on binders.

Binders are made of polymeric materials and account for approximately 5 wt% of the total battery weight [28]. Generally, they are electrochemically inactive. They serve multiple functions: (1) providing stability to the battery; (2) ensuring homogeneous coating and adhesion of the active materials to the current collector; (3) providing an electrochemical window that prevents chemical reactions between the binders and electrodes; and (4) allowing electron and ion movement [29–31]. Binders are crucial for the electrode fabrication process because they are mixed with the electrode material to form a paste. This paste is subsequently coated onto the collector using the doctor blade technique and then dried [20,31]. Throughout the lithiation and delithiation processes, the volume changes in the electrode can damage its mechanical structure. Therefore, the binder used for electrode fabrication must possess sufficient mechanical properties, such as strength, elasticity, flexibility, and hardness, to maintain the integrity of the electrode [27]. Furthermore, the lowest unoccupied molecular orbital (LUMO) of the binder used in the anode should be positioned higher than the chemical potential of the active material. Alternatively, the highest occupied molecular orbital (HOMO) of the binder should be lower than the chemical potential of the cathode [27].

In recent years, numerous reviews have focused on binders. However, this comprehensive review emphasizes aqueous binders and various binder strategies to improve their utilization in batteries. Understanding the failure mechanisms of binders can aid in the development of improved binders, which is another focus of this review.

2. Binders for LIBs and SIBs

The field of LIBs initially exhibited potential when Whittingham along with Michel Armand discovered the “intercalation mechanisms”. Exxon further commercialized the use of Li ions in the layered structure of TiS_2 in the 1970s [32–35]. Within a few years, in the 1980s, Prof. Goodenough provided a breakthrough in Li-ion batteries by discovering a new cathode material, $LiCoO_2$ (LCO), which has a theoretical capacity of 273.8 mAhg^{-1} [36,37]. In 1987, Akira Yoshina of the Ashahi Kasei Corporation introduced the use of polyacetylene as an anode for LIBs [38,39]. This led to the commercial breakthrough of LIBs, which were developed by Sony Corporation in 1991 with LCO as the cathode material and coke as the anode material, exhibiting a cell potential of 3.7 V and an energy density of 80 Whkg^{-1} [40–42]. Since then, there have been several modifications and studies on the cathode, anode, and electrolyte materials of LIBs to enhance their energy density.

Sodium ions are larger (1.02 \AA) than lithium ions (0.76 \AA) and have a higher standard electrode potential (-2.71 V vs. SHE compared to -3.02 V vs. SHE for lithium). Owing to these properties, SIBs have lower energy densities than LIBs [18,43]. The investigation of the potential of sodium in rechargeable batteries began with the insertion of sodium into TiS_2 at room temperature in 1980 [44]. The electrochemical properties of Na-containing layered oxides (Na_xCoO_2) were first reported in 1981 [45]. A significant turning point in SIB research occurred in 2000, when Stevens and Dahn demonstrated a high reversible capacity of 300 mAhg^{-1} using hard carbon in a Na cell, despite its inadequate cyclability for practical battery applications [46]. Subsequently, Okada et al. made another crucial discovery when they reported the electrochemical activity of $NaFeO_2$ in Na cells based on the Fe^{3+}/Fe^{4+} redox coupling [47]. Over the years, efforts have been made to enhance and unleash the potential of SIBs to meet increasing energy demands. In this section, we focus on the binders used in the two technologies.

Binders are essential for improving battery capacity because they affect the surface chemistry of electrodes. The solid electrolyte interface (SEI) and passivation layers formed on the surface of anode materials are influenced by binders [28]. Hence, understanding the chemistry of binders is crucial to developing high-energy-density batteries. Depending on the solubility of the binders in the solvents, they can be classified as aqueous or non-aqueous binders [20,48]. The following subsection discusses in detail some of the commonly used aqueous and non-aqueous binders.

2.1. Non-Aqueous Binders

2.1.1. Poly (Vinylidene Difluoride) (PVDF)

PVDF, a thermoplastic fluorinated polymer, is a widely used non-aqueous binder that has dominated the market for a long time. Its good electrochemical stability (up to 5 V vs. Li⁺/Li) [49], inert behavior toward acids and bases, high mechanical stability, high thermal expansion rate, and excellent processability make it a perfect candidate for use as a binder [50,51]. Understanding the interactions of PVDF in different pH environments is crucial for optimizing electrode slurries. PVDF is stable in acidic (low pH) environments but reacts strongly to alkaline conditions. When exposed to high pH levels (pH ≥ 11), PVDF undergoes a dehydrofluorination reaction, where hydrogen fluoride (HF) is released, leading to the formation of C=C double bonds or crosslinking between polymer chains. This chemical change is like the effects seen in thermal degradation [52]. Despite its favorable properties, PVDF has several drawbacks, including difficulty in recycling, high cost, and toxicity concerns associated with its manufacturing process. PVDF production occurs via two main processes: emulsion and suspension polymerization. The manufacturing of PVDF involves the use of an organic dipolar aprotic solvent, N-Methyl-2-pyrrolidone (NMP), or a polar aprotic solvent, dimethylformamide (DMF) [53], which is highly hazardous to the environment [54–58]. The use of NMP at the industrial scale is restricted by the Registration, Evaluation, and Authorization of Chemicals (REACH) regulation of the European Union [59,60]. Although PVDF has traditionally been employed as a binder for both positive and negative electrodes in commercial LIBs, its effectiveness in Si anodes has been questioned [61]. Weak van der Waals interactions between conventional PVDF binders and Si-based particles result in delamination of the active electrodes from the current collector during cycling, leading to structural fractures that are detrimental to battery performance [62].

The viscosity of oil-soluble binders, type of solvent, molecular weight, amount of binder utilized, and quantity of coupling agent are some of the factors that affect the performance of PVDF homopolymer binders in LIBs. Moreover, PVDF is unstable in the presence of lithium salts, leading to cost concerns and disposal issues [63]. The solubility of PVDF binders in organic-based electrolytes and their susceptibility to swelling, especially in carbonate-based electrolytes, pose challenges to electrode stability and electrochemical performance. The swelling rate of PVDF electrodes worsens at high temperatures (over 60 °C) and can reach 80%, which can have a negative impact on electrochemical performance and cause a noticeable increase in weight [64]. When paired with a carbon-based electrode, PVDF reacts with lithium metal and lithiated graphite (Li_xC₆), resulting in a heat release that can initiate thermal runaway [65]. While operating under extremely cold conditions (−40 °C), the PVDF electrode approaches the glass transition temperature (T_g) (−35 °C), resulting in a deviation from its initial traits of high flexibility and resistance to cracking, transforming it into a rigid and fragile state [66]. Owing to the environmental and cost concerns associated with PVDF, efforts are underway to find alternative binders for LIBs that are both eco-friendly and cost-effective.

The excellent properties of PVDF binders that make them suitable for LIBs do not translate effectively to SIBs for several reasons: (1) The weak binding forces between PVDF and the active material fail to accommodate the substantial volume changes occurring between particles during cycling, resulting in electrode fracture and interruption of the electrical circuit [67,68]. (2) Insufficient passivation during sodium insertion results in PVDF decomposition and fluoride production [46]. (3) The formation of an NaF layer due to the reaction between sodium and fluoride causes the binder to lose its ability to integrate and bind effectively [69]. Research conducted by Vogt et al. revealed that adding fluoroethylene carbonate (FEC) can help mitigate the formation of an NaF layer, which tends to develop in PVDF-based electrodes for SIBs. By reducing NaF formation, FEC can enhance the overall performance and longevity of PVDF-based electrodes used in SIBs [69].

2.1.2. Polyacrylonitrile (PAN)

The functional nitrile groups ($\text{C}\equiv\text{N}$) of PAN make it a suitable binder for LIBs. They have long been employed as matrices in polymer electrolytes owing to their high polarity, stability, high melting point, good mechanical strength, and wide electrochemical windows [29,70–72]. Additionally, PAN exhibits high conductivity and flame resistance at low and high temperatures, respectively [29]. Its high concentration of nitrile groups ($\text{C}\equiv\text{N}$) enhances Li^+ transfer and promotes effective contact between active materials by facilitating interactions between lithium ions and active materials through hydrogen bonds and dipole–dipole interactions [73–77]. Furthermore, PAN has the lowest occupied molecular level (-8.85 eV) and antioxidant properties owing to the C-N group, which is one of the strongest electron-withdrawing groups [78].

Like PVDF, PAN-based electrodes involve the use of NMP solvent for electrode preparation [73]. Compared to PVDF electrodes, PAN-containing electrodes exhibit higher coulombic efficiencies (CEs) because of their binding capabilities. These binding properties also inhibit electrolyte decomposition and facilitate Li^+ diffusion. PAN is widely used in the fiber sector because of its easy synthesis and semi-crystalline structure, which provide certain properties, such as stiffness, hardness, thermal stability, and resistance to organic solvents. The strong interaction between the nitrile groups makes PAN a deterrent to organic solvents [73]. Furthermore, thermal treatment of PAN above 300°C enhances its mechanical properties through the cyclization of the PAN molecule.

The electrochemical performance of PAN was investigated and compared with that of a commercial PVDF binder when applied to a 4.5 V HV-LCO. In this experiment, PAN exhibited high moisture tolerance, an ultrahigh mechanical modulus (8.01 GPa), and a hardness of 381.45 MPa in the liquid electrolyte. PAN uniformly covered the surface of the active material, forming a thin and effective SEI. The formed SEI layer suppressed the decomposition and oxidation of the liquid electrolyte. Furthermore, the author tested the PAN binder in a higher cutoff voltage LCO-based LIB (4.6 V), which demonstrated good capacity retention for up to 50 cycles [78].

The appealing characteristics of PAN make it a suitable choice for use in negative electrodes, such as those made from graphite, silicon, and lithium titanate ($\text{Li}_4\text{Ti}_5\text{O}_{12}$, LTO) [73]. Umirov et al. developed a new anode binder, silane-incorporated cyclized PAN (Si-PAN), using a simple azide–nitrile click reaction. The chemistry behind the reaction and the volumetric expansion of the Si alloy in the Si-PAN binder are shown in Figure 2. Based on the amount of silane in PAN, the study assessed the CE and capacity retention of each electrode cured at 300°C . Among the silane-treated PAN samples, the Si-PAN-2.0 electrode exhibited the highest capacity retention of approximately 60% after 30 cycles [79].

However, the application of PAN as a binder in SIBs is limited. It has been primarily used to create carbon nanofibrous webs for anode-free SIBs [80]. Campeon et al. conducted a study to evaluate a copolymer grafted onto poly(vinyl) alcohol (PVA-g-PAN) as a binder with Ti-based layered oxides, exploring its potential as a negative electrode material for SIBs. PVA-g-PAN exhibited remarkable chemical stability and outstanding electrochemical performance [81].

2.2. Aqueous Binders

Aqueous-based binders offer several advantages, such as cost effectiveness, environmental friendliness, and less stringent processing requirements for air and humidity. Among these advantages, eco-friendliness stands out the most because these binders do not require the use of harmful NMPs. Figure 3 shows the advantages of aqueous binders over non-aqueous binders throughout the electrode preparation process. Additionally, they exhibit rapid solvent evaporation. Compared with traditional PVDF-based binder electrodes, aqueous binder-based electrodes use a smaller quantity (approximately 5%) of the binders, thus enhancing the energy density of the cell. Another significant benefit of aqueous binders is their lower average swelling tendency in carbonate-based electrolytes compared with conventional non-aqueous binders. Furthermore, aqueous binders are more

economical than their counterparts, making the fabrication process more cost-effective [20]. Zeon Co., Ltd. is a pioneering Japanese company in the development of water-based binders [29]. Over the years, several aqueous binders have been explored, including polytetrafluoroethylene (PTFE), styrene–butadiene rubber (SBR), chitosan, lignin, polyacrylic acid (PAA), and sodium alginate (SA), as demonstrated in Figure 4.

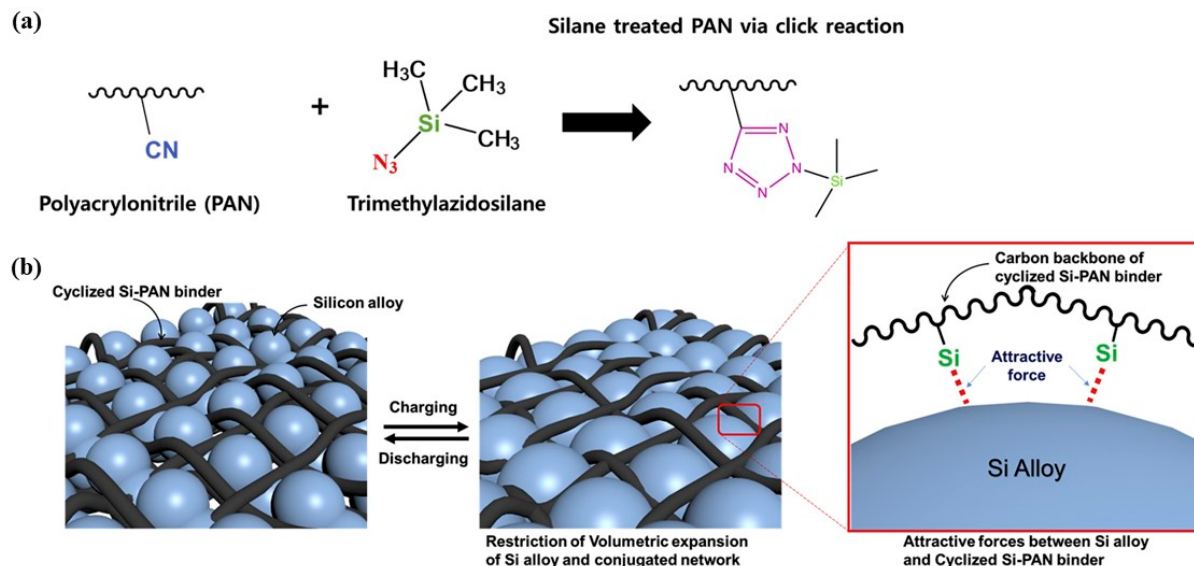


Figure 2. (a) Illustration of the click reaction between azide and nitrile to create Si-incorporated cyclized PAN (b) Demonstration of the expansion of Si alloy when paired with Si incorporated PAN. With permission from [79].

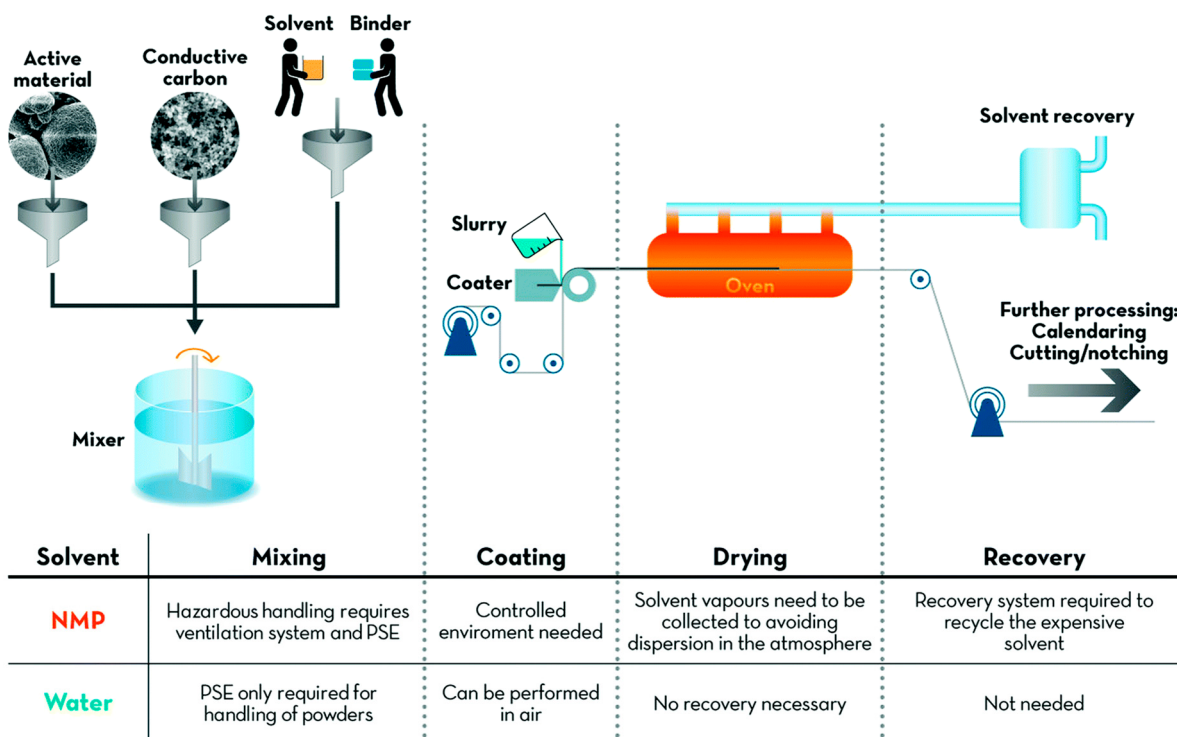


Figure 3. A simplified schematic representation of the production process for batteries. The primary benefits of using water instead of NMP are outlined for each stage, starting from the left and going rightward: the initial mixing of slurry, coating on the current collector, drying of the electrode layer, and solvent recovery. With permission from [82].

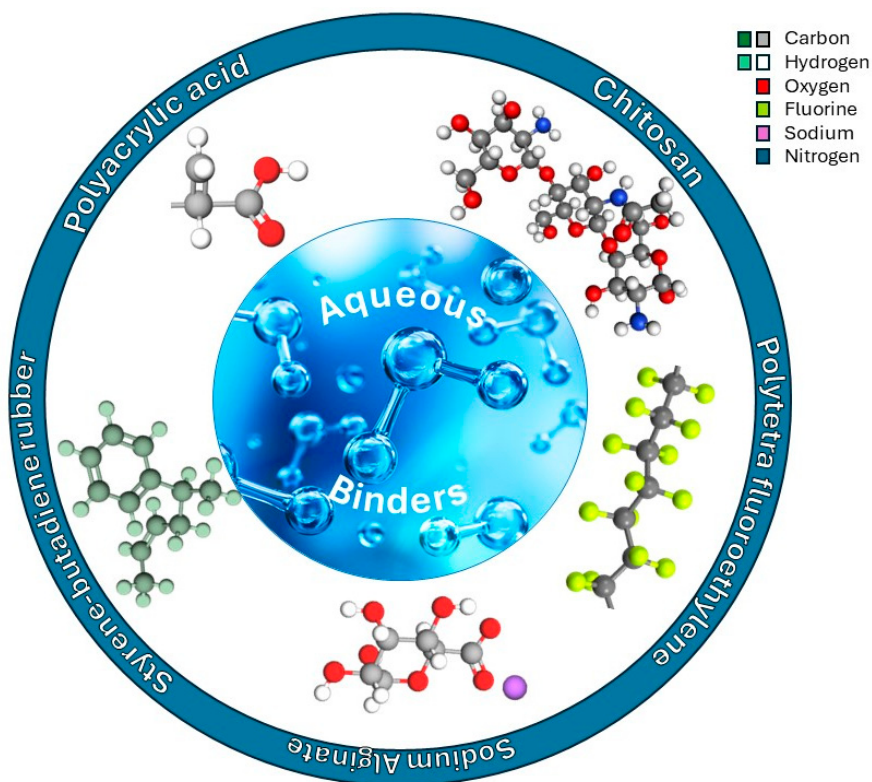


Figure 4. Illustration of the various aqueous binders available in the market for rechargeable batteries and discussed in this review article.

2.2.1. Polytetrafluoroethylene (PTFE)

PTFE is recognized for its environmental friendliness, as it utilizes a water solvent and poses no health risks. It has high chemical resistance, high hydrophobicity, a wide temperature range, insulation properties, UV resistance, weather resistance, a low friction coefficient, fracture and flexural resistance, fire resistance, and minimal water absorption [83,84]. These properties result from its high crystallinity, molecular weight, and unbranched structure, characterized by significant C-F bonding energy (485 kJ mol^{-1}) [85,86]. Although PTFE is associated with a capacity loss in carbon electrodes, these characteristics make it a better binder compared with PVDF. Owing to its superior crystallinity, high post-sintering percentage (>97%), and fiber-forming capacity, it can be considered a suitable binder, especially for LIBs [87–89]. The hydrophobic nature of PTFE facilitates its dispersion in aqueous solutions.

Compared with other polymers, PTFE is less resilient and more flexible. It also has a moderate tensile strength and high elongation at break, which make it appropriate for solvent-free processes and polymer fibrillation techniques [85,86,90]. The fibrillation characteristics of PTFE aqueous dispersions offer an excellent binding capacity with electrode materials, although excessive fibrillation may prevent homogeneous dispersion, leading to poor interconnection with electrodes. The incompatibility of active materials with water and stabilizers presents further challenges, as the PTFE binder relies on an aqueous solvent and stabilizer for the electrode construction process [20,91]. Gao et al. used PTFE as an aqueous binder instead of the organic binder PVDF to fabricate an LFP/C cathode as depicted in Figure 5. The cell incorporating the PTFE binder demonstrated an increased discharge capacity of 161.1 mAh g^{-1} and lower shear rate compared with PVDF. Notably, the interfacial resistance (R_{ct}) of the PTFE cell was lower compared to that of PVDF, with values of 21.4 and 28.9Ω , respectively [92].

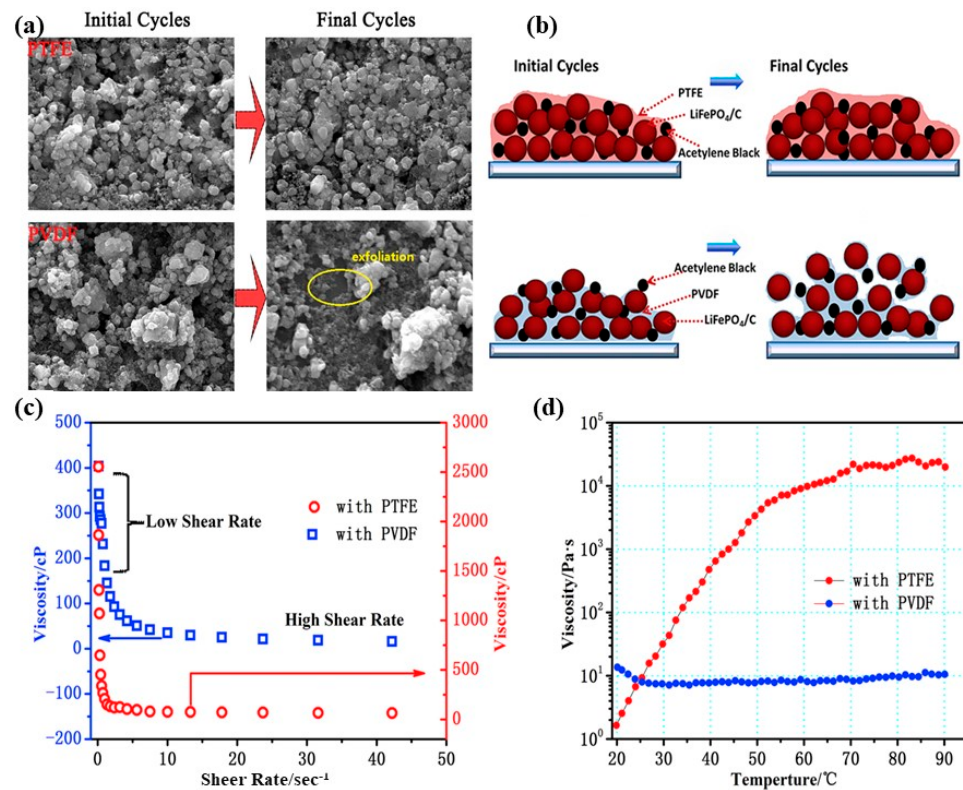


Figure 5. (a) Illustration of the morphology of LFP/C electrodes and (b) the schematic view of electrodes with PTFE and PVDF in initial cycles and in final. Viscosity of the slurry prepared using PVDF and PTFE binders (c) at the room temperature and (d) at temperatures ranging from 20 °C to 90 °C. Reproduced with permission from [92].

2.2.2. Styrene–Butadiene Rubber (SBR)

SBR is produced through the synthesis of 1,3-butadiene and styrene monomers, and its characteristics depend on its molecular structure, including the ratio of styrene to butadiene, degree of cross-linking (DoCL), type of emulsifier, and polymerization temperature [20,93]. Compared with PVDF, SBR is a better elastomer because it is more flexible, has better binding properties, and can withstand higher temperatures [94–97]. Zeon Co., Ltd. is a prominent manufacturer of SBR binders for both anodes and cathodes [20].

SBR is generally used as a binder in combination with carboxymethyl cellulose (CMC). Within the SBR/CMC system, SBR plays a significant role as a binder, while CMC regulates the dispersibility and viscosity of the slurry [98]. In graphite anodes, SBR provides flexibility to the SBR/CMC system, which tends to become brittle after vacuum drying [99]. The SBR/CMC binder improves the adhesion between the electrode film and current collector, forming an efficient three-dimensional network for electron transport. The SBR/CMC binder also aids in creating a uniform SEI film, thereby preventing the formation of Li dendrites. Zhang et al. used a mixture of SBR/CMC in weight ratios of 1:1, 1:3, and 3:1 as a binder for a ZnFe₂O₄ (ZFO) electrode in LIBs. The 1:1 configuration achieved a discharge capacity of 873.8 mAhg⁻¹ after 100 cycles at a 0.1 C rate, exhibiting a minimal capacity fading rate of 0.06% per cycle (Figure 6a). This indicates the potential of the SBR/CMC binder [96]. However, it has been observed that the SBR/CMC system fails with the Si anode due to its low binding ability with respect to the volume expansion of the Si anode [100]. Even in SIBs, the SBR/CMC binder combination performed better than the other binders. Zhang et al. evaluated the use of an SBR/CMC binder in NASICON-type NaTi₂(PO₄)₃ (NTP) SIB anodes in comparison with CMC and PVDF. The batteries demonstrated a specific capacity of 120 mAhg⁻¹ for 500 cycles at 0.2 C (Figure 6b). The robust adhesive strength and flexibility of the CMC and SBR binder systems facilitate better ionic- and electron-conductive connections [101].

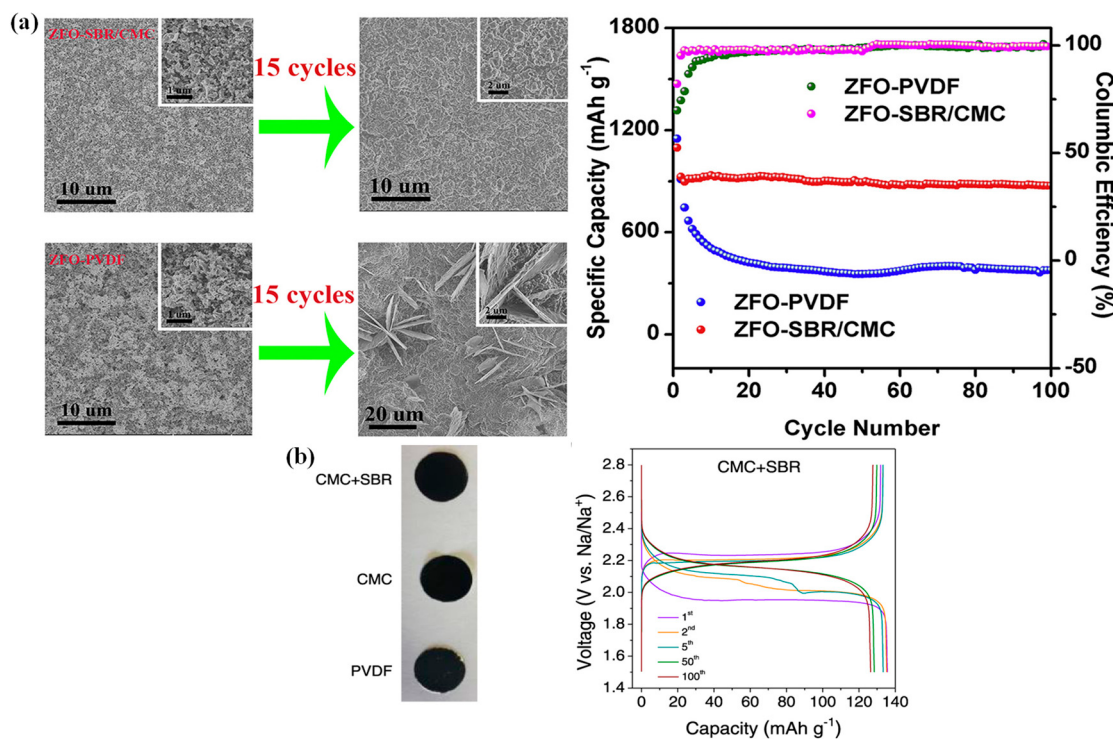


Figure 6. (a) SEM images of ZFO-SBR/CMC and ZFO-PVDF binder. Cyclic performance of the same binder electrode assembly [96]. (b) Photos of NTP electrode slurries made with each of the three different binder mixtures and Galvanostatic charge–discharge curves and cycling stability tests for the $\text{NaTi}_2(\text{PO}_4)_3$ electrode slurries acquired at 0.2 C rate (capacity at 1 C = 133 mAh g^{-1}) over 500 cycles using CMC + SBR system [101]. Reproduced with permission.

The DoCL and the ratio of styrene to butadiene units are two important factors that affect the properties of SBR, including its tensile strength and Tg [99]. To understand the effect of the DoCL on the properties of the SBR/CMC binder, Isozumi et al. conducted a study on LCO composite electrodes by modifying the DoCL within SBRs. They found that SBRs with a lower DoCL exhibited better electrochemical properties [102]. Conversely, Jolley et al. examined the effects of different DoCLs in SBRs on graphite anodes using a CMC/SBR binder system. Their results showed that SBRs with a higher DoCL provide better and more consistent capacity retention than those with a lower DoCL. A higher DoCL content in SBRs also resulted in electrode coatings with stronger cohesiveness, which reduced active material loss and capacity fading over time by reducing delamination between the active material layers [103].

SBR is widely available in aqueous binders due to its strong mechanical properties, making it a preferred choice. When combined with CMC, these polymers work together effectively to meet current binder requirements. Additionally, it has the potential to replace the environmentally harmful PVDF in the market.

2.2.3. Polyacrylic Acid (PAA)

PAA serves as a functional polymeric binder featuring carboxylic acid functional groups ($-\text{COOH}$) that establish weak hydrogen bonds with the surface $-\text{OH}$ groups of the active materials, thereby forming a conductive ionic film [29,104,105]. As a binder, PAA imparts advantages, such as robust binding ability, adhesive strength, swelling properties, high stress at break (90 MPa), and uniform particle distribution within the electrode [51,106,107]. The electrical properties of PAA improve with the increase in molecular weight and higher concentrations of Li^+ , enhancing its overall performance [108,109]. For PAA, a high pH value improves particle dispersion but severely compromises the mechanical properties of the binder [109]. PAA is soluble in both water and NMP, facilitating

strong hydrogen bond formation with the active materials and current collectors because of the presence of carboxylic acid functional groups [51]. PAA also enables regulation of the distance between functional groups by copolymerization with other monomers, thereby facilitating the adjustment of the mechanical characteristics of the binder and its ability to swell and dissolve in an electrolyte solvent [110]. In addition, PAA binders help graphite surfaces establish a consistent and stable SEI layer that effectively blocks direct contact between graphite and the electrolyte, thereby reducing the rate at which the electrolyte decomposes [111]. Moreover, for silicon-based anodes, PAA demonstrates exceptional cycling performance compared with CMC or PVDF [110].

Extensive studies have explored the use of PAA as an aqueous binder in LFP cathodes [112]. The obtained results indicated reduced polarization, lower resistance, and higher reversibility with sustained capacity retention (99.3%) for up to 200 cycles compared to LFP/PVDF cathodes [113]. However, PAA is less effective in lithium nickel manganese oxide (LNMO) electrodes with high mass loadings owing to certain challenges, such as high internal resistance in the initial cycles, which is attributed to several factors, such as contact resistance, inhomogeneous binder distribution, and poor electrolyte wetting. By modifying the polymer chemistry of PAA, problems, such as agglomeration and electrode pore clogging, can be reduced. This modification can be achieved by copolymerizing PAA with various functional groups, which can enhance certain properties, such as adhesion strength, surface chemistry, and electrolyte swelling. This improves the potential of the PAA binder system for LNMO [114].

PVDF and Na-PAA were compared as binders for N-doped hollow carbon nanotube (N-CNT) anodes in SIBs. The electrochemical performance of the N-CNTs was improved by the moderate-molecular-weight Na-PAA binder, which also decreased the internal resistance, generated a homogenous SEI layer, and increased the electrochemical activity. The Na-PAA binder N-CNTs observed an initial CE of 61.2%, delivering a reversible capacity of 175.5 mAhg^{-1} after 300 cycles at 200 mA g^{-1} , compared to PVDF-based N-CNTs [106]. Another study compared PAA and PVDF as SbTe metallic anodes in SIBs. Functional PAA binder significantly enhanced the overall electrochemical performance of these bimetallic alloy electrodes with different carbon contents, leading to excellent capacity retention and cycling stability, particularly notable in the SbTe-C20 electrode, which exhibited an initial CE of 61.2% and delivered a reversible capacity of 175.5 mAhg^{-1} after 300 cycles at 200 mA g^{-1} [115].

2.2.4. Chitosan

Chitosan, primarily composed of β -(1,4)-linked 2-deoxy-2-amino-D-glucopyranose units, is derived from chitin, a natural biopolymer derived from the partial deacetylation of poly(β -(1 → 4)-N-acetyl-D-glucosamine), as illustrated in Figure 7a [116,117]. Chitin has a structure similar to that of cellulose, but with the hydroxyl groups replaced by acetamide groups ($-NHCOCH_3$) [118]. Unlike chitin, chitosan is soluble in dilute aqueous acetic acid solutions, in which the glucosamine unit ($R-NH_2$) protonates into its positively charged form ($R-NH^3+$) [119,120]. Its abundance and the presence of amino and hydroxyl functionalities have rendered chitosan conducive for copolymerization or hybridization with other functional polymers, making it an effective water-soluble binder for various electrode materials [20]. Chitosan was initially introduced as a binder by Chai et al. for a graphite anode, achieving a CE of up to 95.4% [116]. Chitosan has been applied in various aspects of LIBs, serving as a template during active material synthesis, a precursor for carbon coating, a binder for numerous anode materials, and for gel polymer electrolytes [116,120,121].

One study explored the biopolymer chitosan as a promising binder for producing LFP cathodes in LIBs as demonstrated in Figure 7b. Utilizing chitosan as a binder resulted in an electrode with a high discharge capacity of 159.4 mAhg^{-1} , along with an outstanding capacity retention ratio of 98.38% [122]. Several properties dictate the use of chitosan as a binder. The degree of acetylation (DA), which is the percentage of monomeric acetylated units, and the degree of polymerization (DP), which is the number of monomer units in

a biopolymer, are crucial parameters that dictate the chemical and physical properties of chitin and chitosan [123]. Chitosan also has applications in Si anodes; its proposed mechanism is depicted in Figure 7a. Hamzelui et al. evaluated chitosan samples with various DAs and DPs as binders for Si/Gr-based anodes. Electrochemical measurements conducted in Si/Gr || Li metal and NMC622 || Si/Gr full cells led to the selection of a chitosan binder with a high DP of 1618 and a DA of 50% (DA50) as the optimized version for evaluating Si/Gr anodes in battery cells [117].

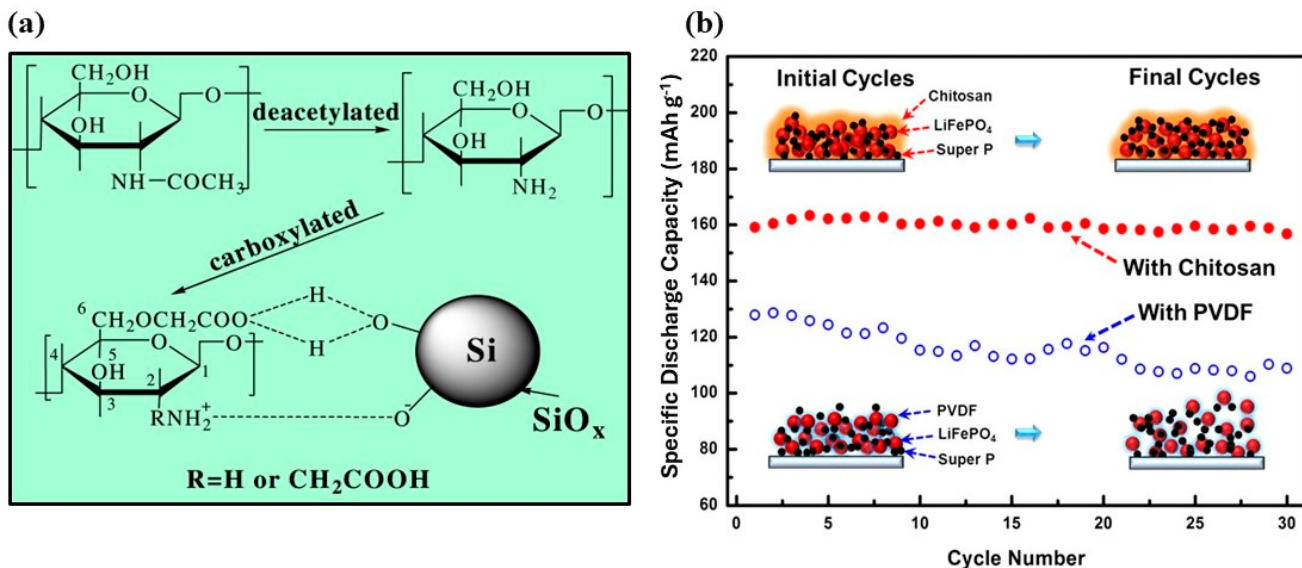


Figure 7. (a) C-chitosan synthesis pathways and proposed C-chitosan bonding mechanism with the Si nano-particles surface [120] (b) Cyclic performance comparison of PVDF and chitosan for LFP cathode [122]. Reproduced with permission.

Gao et al. created a novel polymer network based on cross-linked chitosan as a binder for immobilizing Sb particles on SIB anodes. This cross-linked chitosan structure effectively reduced the negative mechanical impact of the substantial volume expansion. This enhances the electrochemical efficiency of the Sb anode in SIBs. The electrodes demonstrated stable cycling and a charge capacity of 555.4 mAh g⁻¹ at 1 C after 100 cycles, with a capacity retention of 96.5% compared to the initial cycle [124].

2.2.5. Sodium Alginate (SA)

Alginate, a high-modulus polysaccharide, is widely distributed in the cell walls of brown algae and other microorganisms [20,56,125–127]. It comprises copolymers of β -D-mannuronate units (M block) and α -L-glucuronate (G block) linked by 1,4 linkages. Alginate benefits from the presence of metal ions, which enhance its mechanical properties [128,129]. SA, an alginate binder, is commonly used in LIBs and SIBs. Owing to the abundant carboxyl groups in its polymer chains, SA forms strong interactions, such as hydrogen or covalent bonds, with active material surfaces [20]. It dissociates readily in water to generate carboxylic anionic free radicals [130]. SA also exhibits excellent mechanical properties in electrolyte solvents, boasting a stiffness that is approximately 50 times higher than that of PVDF [131].

When used as a binder mixed with a Si anode, alginate demonstrated remarkable electrochemical capacity improvement and cycling stability compared to CMC or PVDF binders [56]. The reversible and self-healing bonds formed in the presence of calcium (Ca^{2+}), or magnesium (Mg^{2+}) ions contribute to extreme toughness and resilience. Alginate, particularly when crosslinked with Ca^{2+} , significantly enhances the cycle stability of Si-based anodes on Cu-foil current collectors [132–135]. The G blocks of alginate specifically bind with Ca^{2+} to create a series of reversible and robust electrostatic crosslinks known

as the “egg-box structure”. The calcium-mediated “egg-box” electrostatic crosslinking of alginate enhances toughness, resilience, and electrolyte desolvation, thus improving its performance as a Si-binder for LIBs, as observed by Yoon et al. [127].

The strong electrochemical properties of alginate enable its use as a binder in MnO_2 graphene sheet cathodes for LIBs and TiO_2 anodes for SIBs [131,136]. The MnO_2 -GS hybrid exhibits outstanding high-rate and long-cycling electrochemical performance owing to the superior contribution of SA. TiO_2 electrodes with SA in SIBs demonstrate electrolyte decomposition, minimized side reactions, heightened electrochemical reaction activity, efficient suppression of polarization, and a favorable electrode morphology. These properties are attributed to the abundant carboxylic groups, high Young’s modulus, and robust electrochemical stability of the SA binder. In this system, the initial CE reached 62% at 0.1 C and achieved a capacity of 180 mAhg^{-1} , with no degradation after 500 cycles at 1 C [136]. In another example, environmentally friendly SA was employed as an aqueous binder in a traditional layered transition-metal oxide cathode, $\text{P2-Na}_{2/3}\text{MnO}_2$, for SIBs. The initial discharge capacity of the electrode with the SA binder was 154.2 mAhg^{-1} [137].

3. Strategies of Novel Binders

3.1. Conductive Binders

Conductive polymers possess elongated pi-electron networks within their backbone structure. Through doping, these polymers exhibited electrical conductivities comparable to those of metallic electron conductors, reaching nearly 10^4 S cm^{-1} [138]. The electrical conductivity of these polymers greatly depends on their oxidation/reduction states; they exhibit high conductivity in the oxidized state and become insulating upon reduction [139]. Using a conductive binder instead of a conventional binder/conductive additive combination leads to a reduced parameter space and minimizes the presence of nonactive components in the electrode formulation [140,141]. The use of a conductive binder can increase the gravimetric density of LIBs. Conductive binders can also suppress or completely prevent capacity losses caused by the physical separation of the active material and conductive phase. However, some conductive polymers have limited solubility in water; hence, organic solvents are necessary for electrode coating. To further increase the use of conductive polymers, Zheng et al. developed emulsion polymerization methods to produce conductive polymer binders in water for Si anodes [142].

Several conductive polymers have been used to increase the efficacy of Si anodes in LIBs. These binders play a pivotal role in holding the active Si particles and securing them to the current collector, as shown in Figure 8. Furthermore, they facilitate the formation of a conductive pathway that is essential for electron transfer [143,144]. One study demonstrated the effectiveness of a SiO electrode, a promising alternative anode material for LIBs, featuring a high concentration (98%) of active SiO and only 2% poly (9,9-dioctylfluorene-co-fluorenone-co-methylbenzoic ester) (PFM) as a conductive binder. The SiO/PFM electrode system demonstrated 500 reversible cycles with a capacity retention of over 90% [140]. Yu et al. introduced an n-type mixed ionic–electronic conductor, polyoxadiazole (nMIEC POD), as a versatile binder for Si anodes. The Si anode with this binder achieved a high reversible capacity of 3079 mAhg^{-1} at 0.6 Ag^{-1} after 200 cycles and maintained a remarkable capacity of 2151 mAhg^{-1} at a high current density of 2 Ag^{-1} even after 500 cycles [145].

In another study, a pyrene-based homopolymer, poly (1-pyrenemethyl methacrylate) (PPy) conductive binder, was used to assemble a graphite/nanoSi composite electrode. This composite electrode exhibited a high areal capacity exceeding 2.5 mAhcm^{-2} during long-term cycling (over 100 cycles) [146]. These conductive binders were inspired by the long-lasting adhesive properties of mussels in wet environments. Poly(3,4-ethylenedioxythiophene): poly (styrenesulfonate) (PEDOT:PSS), a commercially available conductive binder, has been widely studied for applications in LIBs [143]. The use of a PEDOT:PSS binder reduced the use of carbon additives by 3% [139].

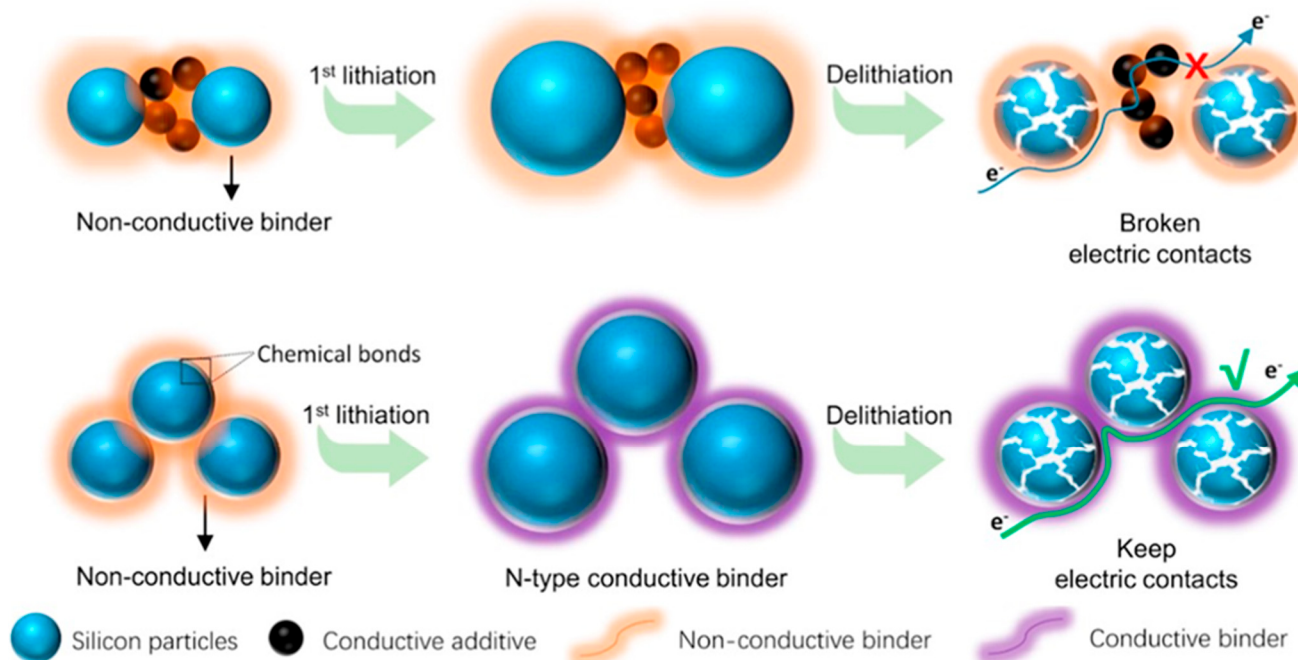


Figure 8. Demonstration of the effectiveness of conductive binders in securely binding Si particles together, compared with non-conductive binders. Reproduced with permission from [144].

3.2. Composite Binders

Composite binders, which consist of a conductive material and a polymer, have two purposes: they improve electrical conductivity and create mechanical adhesion between the electrode components. This dual role is important, particularly under mechanical stress caused by volume changes during the lithiation and delithiation processes [147]. Owing to these benefits, Rao et al. combined lithium polyacrylate (LiPAA), which has a good conductivity attributed to the presence of additional Li^+ ions [148,149], with SA to improve its mechanical properties for LNMO cathodes. The addition of SA effectively mitigated capacity fading [150]. Researchers investigated composite binders of carboxymethyl chitosan (CCTS)/PEO with different mass ratios in the study of $\text{LiNi}_{0.5}\text{Mn}_{1.5}\text{O}_4$ (LNMO) cathodes. The optimized CCTS/PEO composite (85/15, *w/w*) showed slightly better cycling performance than PVDF, retaining 81.4% capacity after 200 cycles at a 0.5 C rate, as opposed to 79.8% for PVDF [151].

Fu et al. investigated the impact of a polymer composite (MPVDF) incorporating maleic-anhydride-grafted polyvinylidene fluoride (MA-g-PVDF) into PVDF as a binder for LCO cathodes in LIBs. Compared to cathodes using PVDF alone, the lower crystallinity of MPVDF led to a 38.5% increase in the battery discharge capacity at 2 C, while also improving the battery capacity retention from 84.5% to 90.2% after 300 cycles at 0.5 C [152]. In addition, a composite binder was successfully synthesized using tapioca starch, a natural water-soluble polysaccharide derived from cassava, and polyethylene glycol (PEG). This composite binder demonstrated improved mechanical characteristics, such as elevated elastic modulus and hardness. Due to improved adhesion between the binder and active Si nanoparticles, Si-starch/PEG electrodes achieved an initial capacity of 3486 mAhg^{-1} with a 70% initial CE [153].

The conductivity of PEDOT:PSS can be further improved using CMC as a binder, as demonstrated by Shao et al. (Figure 9) [154]. Another study developed a water-soluble conductive composite binder consisting of CCTS and PEDOT:PSS as the conductivity-enhancing agent for LFP cathodes in Li-ion batteries. In a 10 Ah CCTS-LFP prismatic cell, testing of the PEDOT:PSS/CCTS binder revealed similar cycling performance, retaining 89.7% of the capacity at 1 C/2 C charge/discharge rates, as opposed to 90% for commercial PVDF-LFP over 1000 cycles [155].

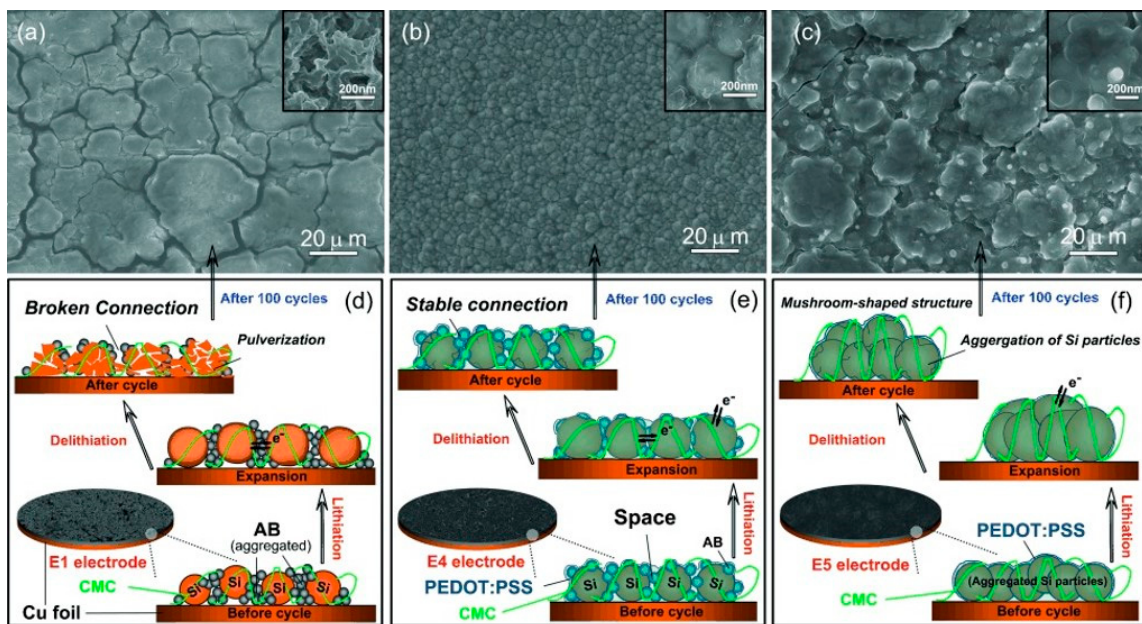


Figure 9. SEM images of different samples with various content of acetylene black (AB) and PEDOT:PSS after 100 cycles. (a,d) contain 20% AB and 0% PEDOT:PSS, respectively, (b,e) contain 10% AB and 10% PEDOT:PSS, respectively, and (c,f) contain 0% AB and 20% PEDOT:PSS, respectively (d–f) represents schematic illustrations of lithiation/dilithiation of the same samples. PEDOT:PSS improves the binding of Si particles compared with cells without the PEDOT:PSS binder. With permission from [154].

Composite binders have also been applied to SIBs. Kim et al. presented a new binder system for antimony-based SIBs, comprising cyanoethyl pullulan (pullulan-CN) cross-linked with PAA. The cyanoethyl groups aid in sodium ion transport, and the pullulan-CN backbone offers mechanical toughness to resist the volume expansion of antimony during sodiation. By maintaining 76% of their initial capacity after 200 cycles of 1 C discharge and 1 C charge, SIB cells using this composite binder showed better cycle life and kinetics. Additionally, they retained 61% of their capacity at 20 C as opposed to 0.2 C [156]. Top of Form

3.3. Self-Healing Binders

To improve the cycling stability of LIBs, a self-repairing binder uses both reversible and non-covalent bonds to mitigate the external and internal damage caused by the large volume changes in Si-based anodes [157]. Self-repairing polymers (SHPs) can repair the damage induced by external stimuli or unwanted cracks, making them suitable for maintaining stable support structures [158–160].

By adjusting the self-repair mechanism and polymer backbone, researchers can modify polymers to attain the ideal properties for their intended use. The self-repair processes can be classified into physical and chemical mechanisms [161]. The self-repair process is usually aided by SHP binders used in electrode systems via dynamic bond interactions at the molecular level [162]. The various reversible interactions at this level encompass both covalent and noncovalent bonds. Covalent bonds, such as disulfide, imine, borate ester, and acyl hydrazone bonds, have been successfully integrated into SHP binders [163–167]. SHP binders relying on non-covalent bonds, including hydrogen bonds, metal-ligand, host-guest, ion-dipole, and $\pi-\pi$ interactions, exhibit lower kinetic stability and weaker dissociation compared to dynamic covalent bonds [168–174]. However, they are also easier to construct. SHP binders based on reversible noncovalent bonds can attain self-repair properties with mobility and flexibility.

Over the years, self-healing binders have been primarily used with Si anodes to advance next-generation high-energy-density LIBs. This preference stems from the significant

challenges faced by Si anodes, including severe pulverization and an unstable solid electrolyte interphase, attributed to the substantial volume change (exceeding 300%) during the cycling process [175]. Poly(ether-thiourea) (TUEG) has a zigzag hydrogen-bonded structure that inhibits unfavorable crystallization and provides exceptional stretchability, self-healing characteristics, and appropriate viscoelasticity. Owing to these properties, TUEG can improve the cycling performance of Si anodes. In this study, the utilization of thiourea-based polymeric binders (PAA-TUEG) led to LIBs with increased capacity, prolonged cycle life, and improved rate performance, with an initial CE of 87.2% and a remarkable cycle life of 2744.3 mAhg^{-1} after 300 cycles [176]. Another study utilized a poly(ether-thiourea) (PET) polymer as a self-healing binder for silicon anodes in LIBs, referred to as SHPET. With the SHPET binder, the resulting Si anode electrode demonstrated remarkable rate capability, achieving approximately 3744 mAhg^{-1} at 0.42 Ag^{-1} and 1917 mAhg^{-1} at 4.2 Ag^{-1} , respectively, along with excellent cycling stability [177]. In another study, a novel polymeric binder integrating PEG groups into SHP was introduced for Si microparticle-based electrodes in LIBs [178].

Nature has inspired the development of self-healing binders. Drawing inspiration from *Parthenocissus* plants, Wang et al. created a citric acid (CA)-PAA binder for silicon anodes. This binder forms multiple hydrogen bonds through the in situ cross-linking of water-soluble CA and PAA, establishing a reversible network for silicon particles, as illustrated in Figure 10 [179].

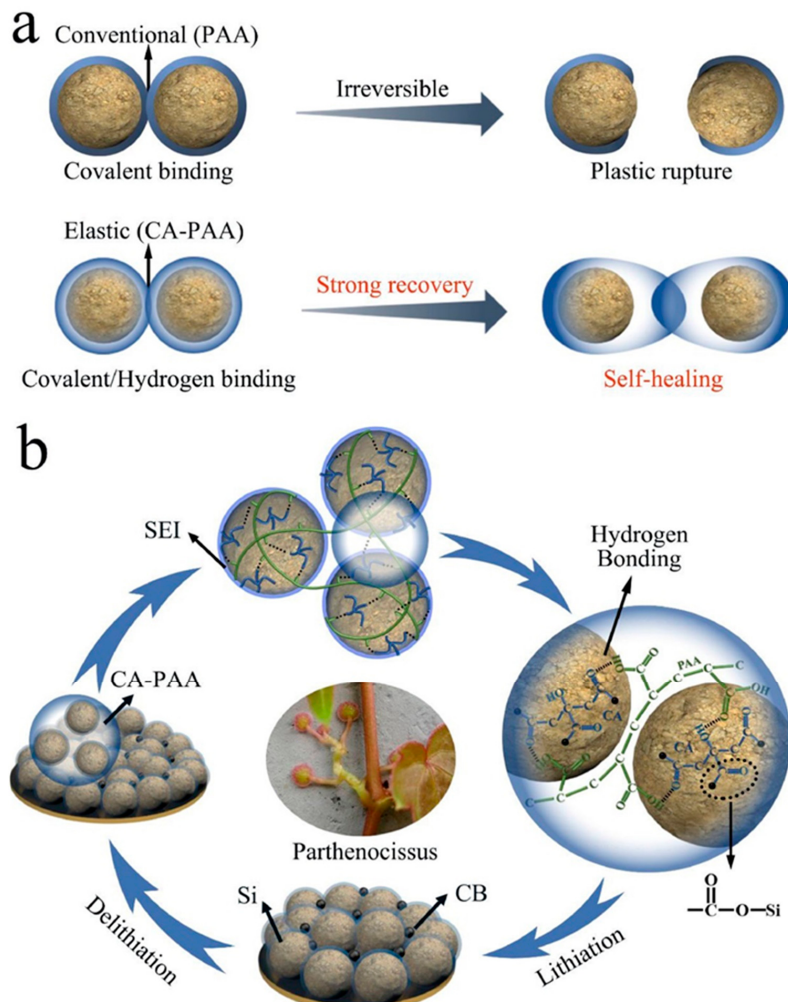


Figure 10. (a) Schematic diagram of the type of chemical interaction between binders and Si particles. (b) Schematic design of the CA-PAA binder, and the chemical bonding between the CA-PAA binder and Si particles. With permission from [179].

4. Binders for SSBs

Traditional LIBs use liquid electrolytes that pose safety risks owing to their low flash points [180,181]. To solve this, scientists have been working on creating all-solid-state batteries (ASSBs), which use inorganic solid electrolytes in place of organic liquid electrolytes. High-potential cathode materials can be used in SSBs because of their improved electrochemical stability, which can lead to an improvement in energy density. These batteries also have advantageous mechanical qualities that add to their general durability and safety [182].

Top of Form

The capacity fading of SSBs is caused by the separation of the active components of the solid electrolytes during cycling. Cracks between solid electrolytes and active materials form as a result of the large strain and stress caused by the significant volume changes that occur during lithiation and delithiation [183]. To address this challenge, polymeric binders are essential for reinforcing the interfacial contact and structural integrity of ASSBs [184,185]. The binder used in SSB electrodes should also meet the following requirements: (1) promote ionic transport at the interface; (2) maintain mechanical integrity while remaining stable over a wide temperature range; (3) resist oxidation or reduction during charge and discharge cycles; and (4) prevent dissolution into the electrolyte or ensure that the solid-state electrolyte remains insoluble in the polymer [185–191]. Connectivity to the conductive network can be facilitated by the functional groups inside the binder molecules, which adhere chemically to the electrode particle surfaces [192]. This binding action of the functional groups enhances electrode contact [193,194]. Furthermore, the long-chain structure of the binder provides additional mechanical resistance to the electrode volume expansion [195]. Hence, binders with abundant functional groups and good chain flexibility are crucial for achieving long-term cycling performance in ASSBs.

The exploration of binders in ASSBs utilizing sulfide electrolytes has been limited because the sulfide electrolyte itself can serve as a binder in the composite electrolyte [185]. Owing to the strong reactivity of sulfide materials to organic solvents, the choice of solvent for wet processing is restricted to nonpolar and weakly polar solvents, such as methyl alcohol, toluene, and xylene [196–200]. Consequently, the availability of polymeric binders, including materials, such as SBR, nitrile–butadiene rubber (NBR), and ethyl cellulose, is highly constrained [185,196,197,200]. Rosero–Navarro et al. presented the first investigation into the effect of binder content on the electrochemical performance of all-solid-state lithium batteries employing a composite cathode with a high active material content ($\text{LiNi}_{1/3}\text{Mn}_{1/3}\text{Co}_{1/3}\text{O}_2$, 89 wt%) covered with a solution-derived solid electrolyte. The use of ethyl cellulose as a binder effectively enhanced the cycle life of this ASSB. A higher capacity retention rate was achieved with the addition of a small amount of binder with 0.5 wt% ethyl cellulose, resulting in a capacity retention rate of 91.7% after ten cycles [185]. Another study investigated varying contents of ethyl cellulose as a binder in a composite electrode system comprising the high-nickel material $\text{LiNi}_{0.8}\text{Co}_{0.1}\text{Mn}_{0.1}\text{O}_2$ (NCM) as the cathode active material and $\text{Li}_6\text{PS}_5\text{Cl}$ as the solid electrolyte, as shown in Figure 11. Compared to electrodes with no binder, those with 0.5, 1, 2, and 4 wt% binder content exhibited initial discharge capacities of 94.6, 111.7, 95.8, and 89.9 mAh g^{-1} , respectively. Additionally, the initial CE of the electrodes with 1 wt% binder reached 66.8%, indicating that the binder effectively reduced the initial irreversible capacity. Consequently, 1 wt% ethyl cellulose served as the best binder for the NCM electrode [188].

To achieve high electronic conductivity, sheet-type ASSBs with solid-electrolyte separators as thin as tens of micrometers are required. These sheets are typically fabricated using slurry casting, scaffold infiltration, and solvent-free dry-film methods [184,201–207]. These methods hold promise for realizing the high-energy-density potential of ASSBs at the battery level; however, they require the use of polymer binders [208]. Fan et al. demonstrated that solvated Li_3PS_4 nanoparticles with monodispersed sizes (<50 nm) can be effectively sintered during a low-temperature desolvation process at 250 °C. Leveraging this attribute of low-temperature sintering, a Li_2S cathode ink was developed using sol-

vated Li_3PS_4 nanoparticles as ion-conductive binders. The sintered Li_3PS_4 nanoparticles not only bind the cathode together but also confer upon it an effective ionic conductivity of 0.09 mS cm^{-1} [209].

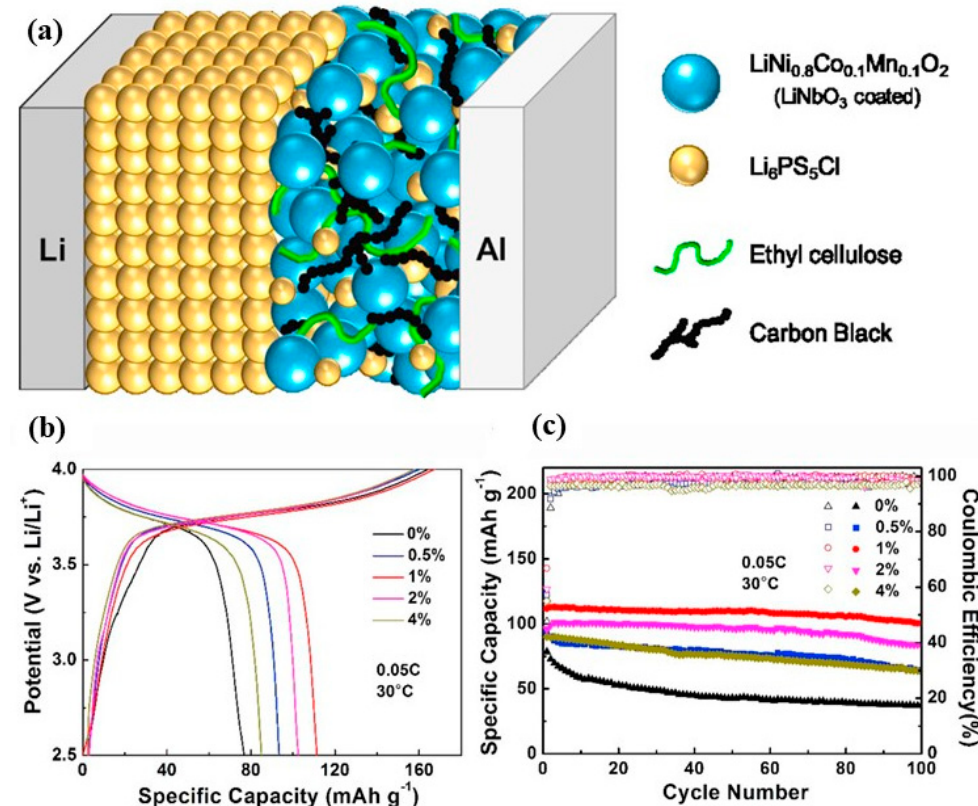


Figure 11. (a) Structure diagram of an NCM/Li₆PS₅Cl/Li ASSB. (b) Initial charge–discharge profiles and (c) cycling performance of cathode composites with different amounts of binder. Reproduced with permission from [188].

Polyethylene oxide (PEO)- or ethylene oxide (EO)- based binders are commonly used in ASSBs because of their good ionic conductivity at elevated temperatures [210–216]. The effectiveness of the PEO family is greatly affected by certain factors, such as salt content, composition of the liquid electrolyte (PEO can react with LiPF₆, particularly at elevated temperatures), and the operating potential of the cathode (PEO typically experiences oxidation beyond 4.0 V) [217]. However, these polymers have drawbacks, such as a low electrochemical oxidation potential and a low melting point, making them unsuitable for 4 V-class ASSBs. Therefore, a suitable binder must be determined to achieve a long cycle life and high performance in high-voltage ASSBs. Liang et al. evaluated the effectiveness of different binders, including PEO, PVDF, and two types of carboxyl-rich polymer (CRP) binders SA and sodium CMC (Na-CMC), for 4 V-class LCO electrodes combined with PEO-based solid polymer electrolytes (SPEs) in assembling ASSBs as illustrated in Figure 12. The electrochemical performance results demonstrated that the ASSBs with SA and Na-CMC maintained 85% capacity after 300 cycles and 59.7% capacity after 1000 cycles, which were significantly higher than those of ASSBs with PEO or PVDF binders [210].

The lists of different binders used in LIB, SIB, and SSBs are mentioned in Table 1. The table aids in understanding the electrochemical performance of these binders in specific electrode systems relative to electrode loading.

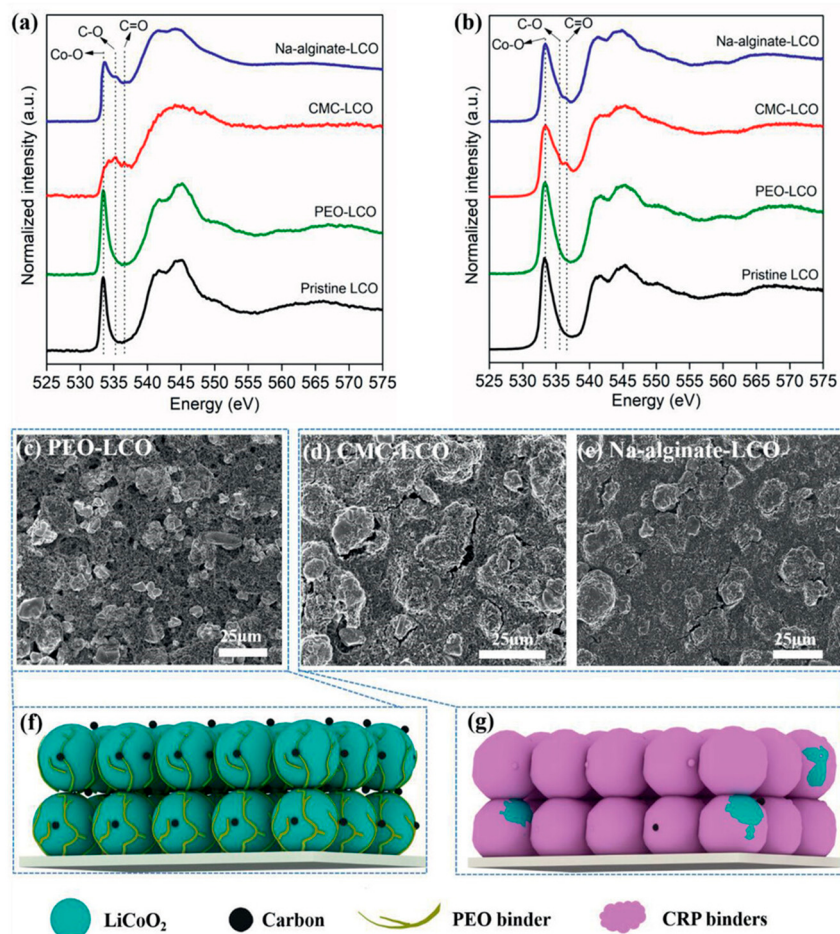


Figure 12. O K-edge X-ray absorption spectroscopy (XAS) in (a) total electron yield (TEY) mode and (b) fluorescence yield (FLY) mode for different LCO samples. SEM images for (c) PEO-LCO, (d) CMC-LCO, and (e) Na-alginate-LCO electrodes. Schematic diagrams for the binding capability and mechanism of (f) PEO and (g) CRP binders. PEO shows better binding capability than CRP binders. With permission from [210].

Table 1. List of various binders used in LIBs, SIBs, and SSBs technologies along with their electrochemical performance.

Binder	Electrode		Battery Technology	Electrode Loading (mg cm ⁻³)	Capacity Retention (%)	Number of Cycles	C-Rate	Specific Capacity (mAh g ⁻¹)	Ref.
	Material	Type							
PVDF	LCO	Cathode	LIB	-	84.5	300	-	-	[152]
PVDF	NMC (111)	Cathode	LIB	6	86.3	200	0.5	111.7	[56]
PVDF Solvay5130	CuO	Anode	LIB	-	30	50	0.2	158.4	[218]
Alginate	NMC (111)	Cathode	LIB	6	89.2	200	0.5	126	[56]
SA	LFP	Cathode	LIB	-	-	50	0.1	165	[84]
SBR/CMC	CuO	Anode	LIB	-	86.85	50	0.2	461.3	[218]
SBR/CMC	ZnFeO ₄	Anode	LIB	3	-	100	0.1	873.8	[96]
SBR/CMC	LFP	Cathode	LIB	-	-	50	0.1	153	[84]
PEO-b-PAN	LFP	Cathode	LIB	-	-	200	0.5	141	[77]
PAN	LNMO	Cathode	LIB	2	85.1	40	0.1	228.2	[219]
PAN-PVDF	LNMO	Cathode	LIB	2	77.5	40	0.1	202.7	[219]
PTFE	Cr _{0.5} Nb _{1.5} (PO ₄) ₃	Cathode	LIB	-	73	20	-	145	[220]
PTFE	Hard Carbon	Anode	LIB	-	80	100	0.05	172	[221]
CMC/PTFE	LFP	Cathode	LIB	-	-	50	0.1	166	[84]
PAA	Si-graphite composite	Anode	LIB	1.5	38.2	300	5	372.3	[222]

Table 1. Cont.

Binder	Electrode	Battery Technology	Electrode Loading (mg cm ⁻¹)	Capacity Retention (%)	Number of Cycles	C-Rate	Specific Capacity (mAh g ⁻¹)	Ref.
	Material	Type						
PAA	LFP	Cathode	LIB	-	-	50	0.1	146.4
NaPAA-g-CMC	Si	Anode	LIB	0.45	79.3	100	0.2	1816
CS-g-PANI	Si	Anode	LIB	0.8–0.9	-	200	-	1091
PVDF	SbTe	Anode	SIB	1.5–2.2	17.9	500	-	49
PVDF	P/C	Anode	SIB	1.5	-	100	1	30
SA/graphene oxide	MoS ₂	Anode	SIB	-	93.1	200	-	336.5
SA/graphene oxide	Na ₃ (VO ₂)(PO ₄) ₂ F	Cathode	SIB	-	95	300	0.5	117.9
SA	Sb-C NP	Anode	SIB	0.6–0.8	-	50	-	553
SBR/CMC	NaTi ₂ (PO ₄) ₃	Anode	SIB	-	90.5	500	0.2	120
PAA-GLY	Sn	Anode	SIB	1.2–1.4	68.4	300	-	377.5
PAA	FeF ₂ -rGO	Cathode	SIB	1.1	-	200	-	120
PAA	SbTe	Anode	SIB	1.5–2.2	55.2	500	-	144
Poly (9,9-diethylfluorene- co-fluorenone-co- methylbenzoic ester)	Sn	Anode	SIB	1.5	-	10	0.1	610
Ethyl cellulose	NMC	Cathode	SSB	4	89.7	100	0.05	100
SBR	NMC	Cathode	SSB	3.5	78.7	45	-	102.5
PVDF-HFP	NMC	Cathode	SSB	4	-	-	0.2	160
NBR	NMC	Cathode	SSB	4	-	-	0.2	149
p(DMAEMA)	LCO	Cathode	SSB	-	89.93	200	0.1	110.6

5. Properties of Binders

5.1. Mechanical Properties

The mechanical properties of binders, such as tensile strength, flexibility, elasticity, and adhesive strength, differ based on the polymer type, molecular structure, configuration, and functional groups [234]. These characteristics are crucial for the ability of an electrode to endure stresses caused by the expansion and contraction of the active materials during charge/discharge cycles. Strategies to achieve favorable mechanical properties in polymers often include improving the intramolecular interactions or boosting the crystallinity [235,236].

5.1.1. Adhesion

Adhesive strength measures the bonding strength between the electrode film and current collector [237]. This property is significantly affected by the molecular weight and functional groups of the polymer [27]. Chemical bonds, like hydrogen or ionic bonds, give binders, such as PAA and alginate, stronger adhesive forces compared to PVDF [235]. This property is used to evaluate the effectiveness of binders because it has a major impact on the electrochemical performance of LIBs [235,238–242]. Binders with high adhesive strength are crucial for maintaining solid connections among the electrode components, even during the volume expansion and contraction that occur during the charge/discharge cycle [235,243–247]. A peeling test is performed to evaluate the adhesion strength of binders.

5.1.2. Tensile Strength

The tensile strength represents the maximum tensile stress that a material can endure before breaking, indicating its resistance to mechanical failure [27,237]. It measures the maximum force that can be withstood without failure and is directly linked to the structural stability provided by the polymer binder [248]. The chemical structure, molecular weight, and crystallinity of polymers influence this property. Higher molecular weight, increased crystallinity, greater crosslinking density, and stronger intermolecular interactions lead to higher tensile strength in the polymers [249,250]. PVDF exhibits low tensile strength, evident from its ability to deform only up to a maximum elongation of 10% [251]. PAA possesses a notable tensile strength of 32.8 MPa when used with LNMO electrode [222].

5.1.3. Elasticity and Flexibility

The key characteristics of binders include elasticity and flexibility, which play a major role in preserving a stable electrode structure in the face of naturally occurring volume changes in a battery [252,253]. Flexibility refers to the ability of a material to bend without breaking, whereas elasticity refers to its ability to return to its former shape after being distorted. Binders exhibiting high levels of elasticity and flexibility, often polymers with low T_g, can better reduce electrode deformation caused by volume changes during charging and discharging cycles [235]. Wang et al. observed that SA (with a stiffness close to 16 GPa) exhibits greater stiffness compared to PVDF when subjected to a silicon anode [254]. PAA-based LNMO electrodes also exhibit a higher elasticity modulus (7.95 MPa) compared to PVDF [222].

5.2. Electrical and Ionic Conductivity

Electrical conductivity in polymers is achieved through a π -conjugated network and free charge carriers [255]. In addition to electrical conductivity, the ionic conductivity of polymers is crucial for the electrochemical performance of batteries. In particular, the power density depends on the movement of the solvated ions through the polymer chains [256]. Factors, such as the degree of crystallinity, porosity, and viscosity of polymers, significantly affect their ionic conductivities [27,257]. In general, the ionic conductivities of polymers are closely related to their T_g values. Polymers with higher crystallinities tend to exhibit lower ionic conductivities because of the lower free volume available for ion transport [258–263]. Other factors, such as the binder affinity with the electrolyte and the electrolyte wetting amount, are also critical in determining the ionic conductivity [242,264]. Structures with high porosity and amorphousness increase the ionic conductivity [27]. Ionic conductivity can occur through specific mechanisms involving functional groups, such as Li-ion hopping [255,265,266]. PEDOT is known to have a high conductivity of 10^3 S cm⁻¹ and, thus, it has great potential as a conductive binder [264]. In a study conducted by Vorobeva et al., PEDOT:PSS/CMC (0.5 S cm⁻¹) showed conductivity five times higher than PVDF (0.11 S cm⁻¹) in LMO electrodes [267]. In comparison to SBR/CMC, PVDF has higher electrical conductivity when used with graphite anodes [268].

5.3. Electrochemical and Chemical Stability

Binders must possess both chemical and electrochemical stability for prolonged periods and through multiple cycles without degrading the energy storage system as demonstrated in Figure 13 [255]. To endure electrochemical reactions and prevent the corrosion of electrolytes during battery operation, binders need to be chemically stable. The surrounding chemical environment, structure, and chemical composition affect stability [27]. Although byproducts from the chemically unstable binders can be used as components of the SEI layer on the electrode surface, excessive accumulation of these byproducts can reduce the CE and negatively impact cycling stability, leading to electrode collapse [235,269].

In terms of electrochemical stability, binders should have reversible redox activity or be redox-inactive, meaning that they should not oxidize or be reduced at highly positive or low potentials. The electrochemical activity of binders can be beneficial for increasing the specific capacity of the electrodes [27]. X-ray photoelectron spectroscopy and Fourier-transform infrared spectroscopy might be used to evaluate these attributes [255].

5.4. Thermal Stability

Thermal properties are critical for both the high-temperature conditions employed in electrode fabrication (such as curing and drying) and the operating conditions [255]. These properties encompass changes in the physical and chemical performance of polymers as heat is applied or removed. Thermal stability is influenced by various factors, such as the strength of binding forces among binders, their compositions, functional groups, primary and secondary structures, the kinetic motion of these structures, and molecular weight [51,270].

Although the typical operating temperature for polymer binders is below 55 °C, they may be exposed to much higher temperatures, often exceeding 100 °C, during manufacturing processes [271]. Furthermore, operational temperatures can unexpectedly increase, making high thermal stability crucial over a wide temperature range [235]. In practice, electrodes must operate effectively in temperature ranges from –20 to 55 °C [272]. Thus, the thermal properties of binders play a vital role in the fabrication and operation of energy-storage devices at elevated temperatures [27]. Comparative studies of different binders on LiMnO₄ indicated that PAA has the highest thermal diffusivity, with a value of $3.1 \times 10^{-3} \text{ cm}^2 \text{ s}^{-1}$, compared to CMC and PVDF, which have values of $1.0 \times 10^{-3} \text{ cm}^2 \text{ s}^{-1}$ and $9.1 \times 10^{-4} \text{ cm}^2 \text{ s}^{-1}$, respectively [51]. However, PVDF has high thermal stability up to 375 °C [273]. Thermogravimetric analysis is a technique used to measure thermal stability and determine the composition of materials [255].

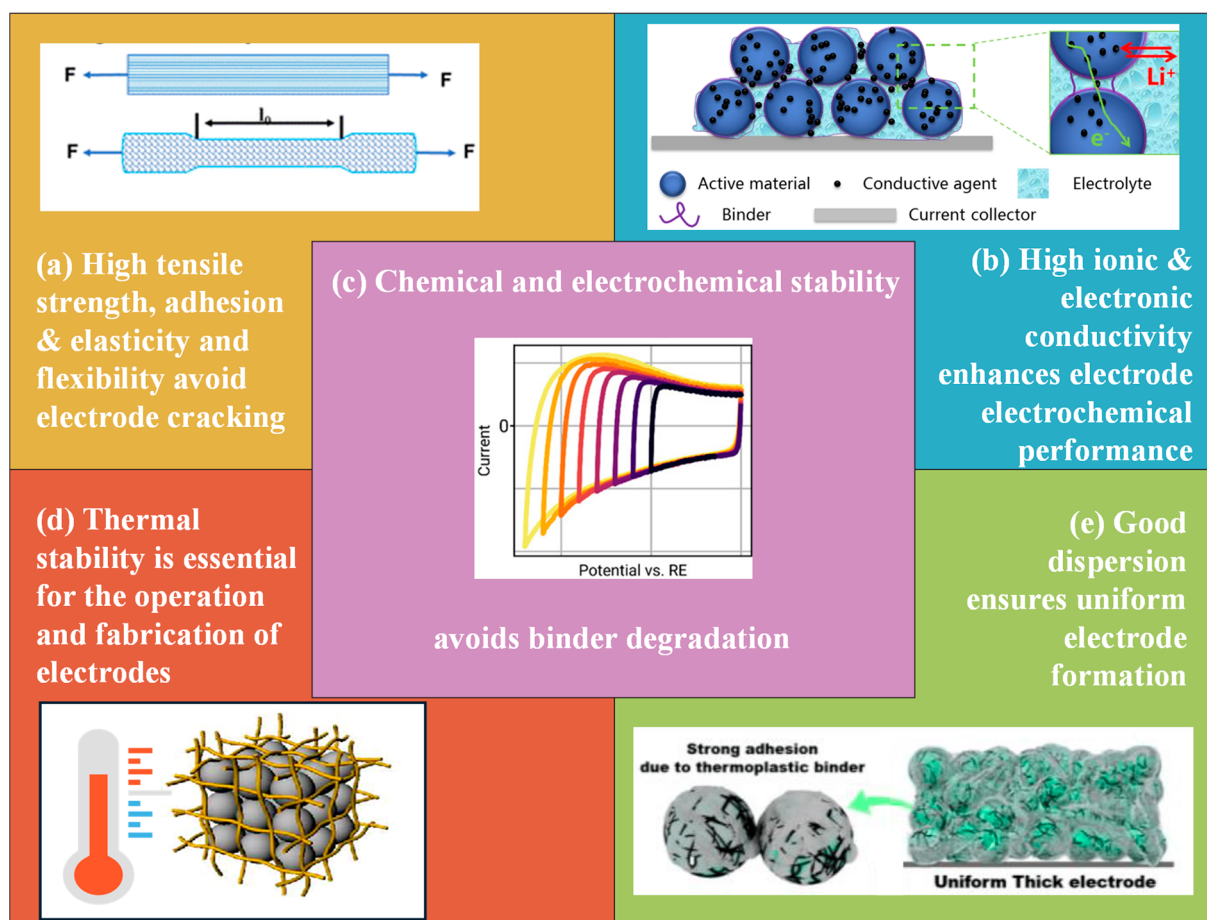


Figure 13. Illustration of the five critical properties associated with binders. **(a)** Mechanical properties, **(b)** electronic and ionic conductivity, **(c)** chemical and electrochemical stability, **(d)** thermal stability, and **(e)** dispersion properties. Reproduced with permission from [11,274–277].

5.5. Dispersion

The ability of polymers to uniformly spread the electrode components within the binder solution to produce a consistent composite is indicated by their dispersion properties. Uniform dispersion can be influenced by several factors, such as the polymer chain structure, charge density, chain flexibility, and mechanisms, such as electrostatic repulsion and depletion [27,278,279]. An uneven distribution of conductive additives, polymer binders, and active materials may have a detrimental effect on electron/ion conductivity, leading to elevated charge transfer resistances (R_{ct}) and localized current overloads [242,264]. Binders containing aromatic components can be beneficial for dispers-

ing carbon-based conductive agents in electrodes due to their $\pi-\pi$ stacking interactions, which facilitate effective dispersion [234].

6. Binder and Electrolyte

Within a battery cell, the electrode is constantly in contact with the electrolyte. The cathode, which has a porous structure, relies on the binder to interconnect carbon particles and form an electron conduction network. The binder also partially covers the surface of the active material, making the distribution and compatibility of the polymer binder with the electrolyte critical for the charge–discharge performance of a battery [280]. The binder must not react adversely with the electrolyte, as such reactions could decompose the electrolyte and negatively impact battery life. A proper swelling rate of the binder ensures good wettability of the electrolyte and prevents the exfoliation of electrode material due to excessive absorption [281]. PVDF, for instance, has a good capability for absorbing electrolytes, which is important for Li^+ ion transport to the active material surface, thus demonstrating good compatibility with electrolytes [282]. The interaction between the binder and electrolyte, along with the wetting amount of electrolyte, is crucial for ion conductivity. While increased wetting can enhance lithium-ion transport, excessive wetting can compromise the adhesive performance of binder and the mechanical strength of the electrode [235]. For solid electrolytes, binders must be soluble in compatible solvents and should not impair ionic conductivity. In a study by Tron et al., six different binder materials, nitrile–butadiene rubber (NBR), hydrated poly(acrylonitrile-co- butadiene) (HNBR), polyisobutylene (PIB), poly(butyl methacrylate) (PBMA), poly(styrene-butadiene-styrene) (SBS), and poly(styrene-ethylene-butadiene-styrene) (SEBS), were evaluated for their suitability with $\text{Li}_6\text{PS}_5\text{Cl}$. NBR and HNBR binders provided good film flexibility, high cohesion, and low adhesion, making them mechanically strong, though they added to the impedance of electrolyte films. PIB and PBMA binders exhibited the highest ionic conductivities at 1.24×10^{-3} and $1.45 \times 10^{-3} \text{ S cm}^{-1}$, respectively. SBS and SEBS offered intermediate performance in terms of ionic conductivity and mechanical properties. The study suggested using binder blends to harness the advantages of different binders for optimal performance [283]. Binders must be compatible with electrolytes to ensure the longevity of batteries.

7. Mechanism of Binders

Bonding mechanisms can be explained through different models, including the mechanical interlocking theory, electronic or electrostatic theory, adsorption or wetting theory, diffusion theory, chemical bonding theory, acid-base theory, and theory of weak boundary layers [284–288]. Mechanical coupling, thermodynamic, and chemical bonding mechanisms are most commonly applied [27,289,290].

A mechanical bonding force is formed between the polymer chains of the binder and the rough surface structure of the electrode. This force is present on the coarse surfaces of all components of the electrode, including the binder polymers, active material powders, conductive agent powders, and current collector foils [29]. This mechanical interlocking mechanism relies on the intertwining of the binder with the surface of the substrate. This mechanism resembles how glue adheres to the uneven wooden surface, as shown in Figure 14a [27,291]. This bonding force can be improved by enhancing the surface roughness and increasing the porosity of each component while selecting an appropriate solvent to effectively dissolve and disperse the binder molecules [14]. This mechanism is commonly observed in PVDF, SBR, and PTFE, where the particles are interconnected with a flexible paste-like material [292]. This also applies to the interaction between PVDF and Si particles, where the stretching of Si particles during lithiation and delithiation leads to their separation and crack formation because this glue-like mechanism cannot hold the Si particles together [289]. According to electrostatic or electronic theory, there is a double electrical layer at the interface between a polymer particle and the metal electrode surface, which dictates adhesion. The adhesion strength is also influenced by the diameter

of the polymer particles [286]. This thermodynamic mechanism is applicable to adhesive polymers lacking chemical binding sites.

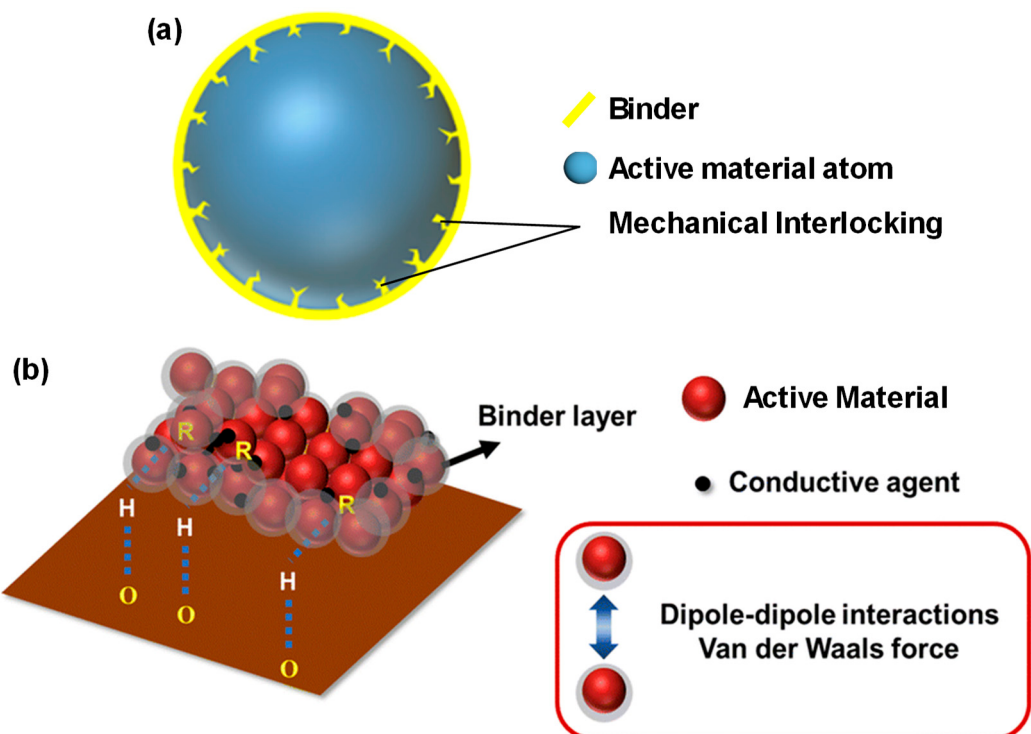


Figure 14. Illustration of the two mechanisms. (a) Mechanical interlocking and (b) chemical mechanisms. Mechanical interlocking refers to the process of securely fastening the binder and the active particles together. Chemical mechanisms entail the interaction between binder particles and active materials through weak forces, such as Van der Waals force. Reproduced with permission from [27,277].

The bond between two closely touching surfaces appears to be best explained by a chemical bonding mechanism. As shown in Figure 14b, covalent, ionic, and metallic chemical bonds are created when atoms share, donate/accept, and delocalize electrons, respectively. This process produces a chemical force that keeps the molecules together. Interfacial forces, such as van der Waals forces, hydrogen bond forces, electrovalent bond forces, covalent bond forces, and coordinate bond forces, occur between the binder and other components of the electrode system. The binder backbone contains numerous polar functional groups, such as $-\text{OH}$, $-\text{O}(\text{C}=\text{O})\text{OH}$, $-\text{O}(\text{C}=\text{O})\text{R}$, $-\text{C}\equiv\text{N}$, $-\text{COOH}$, and $-\text{NH}_2$. These functional groups can interact strongly with the active material or current foil via permanent and induced dipoles between the polar groups or secondary valence forces across the interface, including van der Waals forces [29]. This mechanism was observed in CMC and alginate [292]. For Si electrodes, covalent bonds tend to create permanent bonds between the Si particles and the binder matrix in the electrodes. However, volume changes can lead to stress during permanent binding, resulting in cracking, particularly for Si particles that are affected during the lithiation/delithiation process. Hydrogen bonds form strong but flexible bonds between the binder and electrode particles, making them suitable for electrode materials prone to cracking, such as Si particles [289].

Because of the various bonding interfaces that binders generate with conductive agents, current collector foils, and abrasive active particles, understanding the mechanism of binders in LIBs is difficult. These interactions frequently occur concurrently, making analysis difficult. Furthermore, the mechanism and bonding strength of binders in LIBs are significantly influenced by surface properties, such as surface free energy, elemental

composition, functional groups, chemical/electrochemical reactivity, particle size, and adherent roughness [29]. Top of Form

8. Binder Failure Mechanism

Failure of the binders in battery electrodes can have severe effects on battery performance. A critical function of binders in battery electrodes is to prevent delamination. If the binder is weak, it can lead to electrode delamination, which in turn affects battery performance. Typically, adhesion failure occurs through one of three main mechanisms: destruction of the contact interface, rupture of the binder, or breakage of the adherend. The term “contact interface destruction” describes the separation of the adherend and binder, as well as the loss of adhesive strength. “Adherend breakage” denotes the fracture of the electrode material, whereas “binder rupture” refers to the breaking down of molecular bonds within the binder itself, as seen in Figure 15 [293].

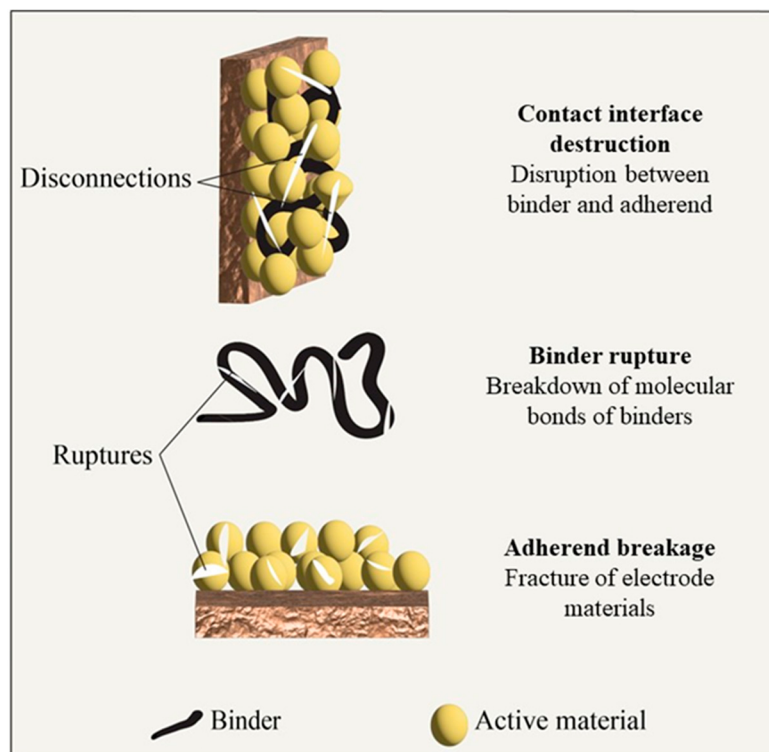


Figure 15. Depiction of three types of binder failure mechanism—contact interface destruction, binder rupture, and adherend breakage.

Loss of contact between the binders and adherends may occur because of the absence of active sites. This loss can result from the different linear thermal expansion coefficients of the organic binder and the inorganic particles. The internal stress generated during heating or cooling can cause the binders to peel off, leading to fractures or breakages in the electrodes. The formation of a weak layer between the electrodes and binders may occur because of impurities and small molecular components, such as plasticizers, stabilizers, residual monomers, and other additives in the system, which tend to accumulate and concentrate at the interface between the binder and the active material. This weak layer is a significant contributor to poor battery performance [29].

Electrode fracture is triggered by several factors. One key cause is the stress field that forms within the crystalline particles and cracks. This stress field can generate debonding forces between the binder and particles. Bulk binding capability is one of the factors contributing to these forces and can be diminished by prolonged contact of the binder with organic electrolyte solutions during storage or battery cycling [29]. When the binder absorbs carbonate solution, its polymer molecular chain swells, causing it to lose its adhesion

capacity after repeated cycling [238,294–299]. Foster et al. suggested that when binders swell upon absorbing an electrolyte, they create significant tensile stress on the surfaces of the electrode particles. These stresses run parallel to the current collector and separator, indicating that binder swelling-induced delamination is likely to occur along these planes. Another contributing factor to electrode fracture is the lack of effective binding sites, which prevents the binder from fulfilling its primary role [299].

Enhancing the structural design to improve adhesion can be achieved by adding functional groups that have stronger interactions with the interfaces. These interactions include hydrogen bonds, Coulombic attraction, and π - π stacking, which offer greater binding strengths than van der Waals forces [134,300–303]. By replacing the weaker van der Waals interactions with more robust connections, the adhesive capacity and overall stability of battery electrodes can be increased [293].

Because of the failure mechanisms linked to binders, along with their inadequate insulation and the reduced gravimetric density of batteries owing to the additional weight of the binder, researchers have been investigating alternatives to conventional binder-based electrodes, such as binder-free electrodes [304–311]. Chemical vapor deposition, vacuum filtration, hydrothermal/solvothermal processes, aerogel production, 3D printing, electrospinning, and electrophoretic and electrochemical deposition are the key approaches used to create binder-free electrodes [312]. However, these binder-free strategies do not resolve all associated challenges. A significant hurdle remains in constructing a binder-free energy storage device that can achieve high energy density, remarkable stability, and substantial mass load ($>10 \text{ mg cm}^{-2}$), which is necessary for commercial applications. In addition, these techniques are still in the experimental phase and require further research to determine whether they can be scaled up to surpass traditional methods.

9. Commercial Viability of Binders

As the battery market continues to expand, the demand for binders is expected to rise accordingly. In 2022, the market for binders used in lithium-ion batteries (LIBs) was valued at USD 1.6 billion, and it is projected to grow to USD 3.7 billion by 2028, with a compound annual growth rate (CAGR) of 18.7% [313]. In 2023, Asia dominated the binder market with 40% of the market share, driven by countries including China, Japan, and South Korea. Meanwhile, North America is experiencing significant growth in the binder market as well as in the battery industry overall [314]. A significant driver of this growth is the increasing adoption of aqueous binders. While PVDF is widely used in commercial applications, there is substantial research in both academia and industry aimed at developing aqueous-based binders. One of the primary drawbacks of PVDF-based electrodes is the use of NMP (N-methyl-2-pyrrolidone), which requires significant energy and the use of a volatile organic compound (VOC) for removal during the drying process [315]. Additionally, the production cost of PVDF is relatively high, at approximately EUR 15–18 per kilogram [55]. In contrast, aqueous binders eliminate the need for NMP, making their production costs significantly lower. The cost of water is less than USD 0.02 per liter, compared to NMP, which costs between USD 1 to USD 3 per liter [316]. According to Wood et al., for a model LIB cell, processing electrodes with aqueous binders is 26 times less expensive than using the conventional NMP-based method, primarily due to the substantial cost savings from omitting the energy-intensive solvent recovery process. This economic advantage, along with environmental benefits, is driving the shift towards aqueous binder systems in the battery industry [315].

Despite ongoing advancements in aqueous binders, the emergence of binder-free electrodes has the potential to diminish the necessity for scaling up binder production. The innovation of binder-free electrodes compensates for the lower energy density typical of binder-based electrodes. Additionally, binder-free electrodes offer enhanced ionic and electrical conductivity [305]. Consequently, the growing emphasis and research focus on binder-free electrodes could reduce the imperative to scale up binder production.

10. Conclusions and Outlook

This review focuses on the crucial role of binders in battery electrode assembly and emphasizes the increasingly reduced use of toxic chemicals, such as NMP and DMC, which are commonly used in the preparation of non-aqueous binders, such as PVDF and PAN. This review investigates aqueous binders, including natural alternatives, such as chitosan, to address safety and environmental problems.

Understanding the mechanics behind the interactions between the binders and electrodes is essential for developing binders that fulfill their functional requirements. This review describes three fundamental mechanisms that explain interactions between binders and electrode surfaces: (1) mechanical interlocking; (2) interfacial forces; and (3) thermodynamic and wetting mechanisms. Although these mechanisms can effectively describe binder interactions, more research is required in this area. The failure mechanisms associated with binders, such as contact interface destruction, rupture, and adherend breakage, require further exploration to improve binder design and durability.

This review also discusses the properties of binders that can aid in the development of better binder strategies. Among these strategies, composite, conductive, and self-healing binders were investigated. Each strategy has its own benefits, such as composite binders that combine the strengths of conductive polymers with traditional insulating binders, self-healing binders that can repair damage during cycling, and conductive binders that eliminate the need for conductive additives. Embracing these new design approaches can help address the increasing demand for batteries with higher energy densities and greater durability.

This conclusion and outlook highlight the importance of advancing binder technology to meet the evolving demands of energy storage. We could approach this objective by learning more about the mechanics behind binder–electrode interactions and by investigating creative binder design techniques. We also discuss a comprehensive understanding of the binder failure mechanisms, which are critical for achieving a higher energy density and improved battery performance. Further research in these areas is critical for developing effective and efficient energy storage systems.

Author Contributions: M.S. designed the structure of the review and wrote the review manuscript and prepared the graphics. M.S. and A.K.M.R. collected papers related to the topic of the review. A.K.M.R., K.Z. and M.S. finished the language polishing and corrections. All authors have read and agreed to the published version of the manuscript.

Funding: This review paper was made possible through the generous financial support of Concordia University, AI-Mogul.

Data Availability Statement: All data utilized in this paper can be accessed through the respective citations provided.

Acknowledgments: We extend our deepest gratitude to AI-Mogul (Montreal, QC, Canada) and Innovee (Montreal, QC, Canada) for their generous support, which was instrumental in the realization of this work.

Conflicts of Interest: The authors declare no conflicts of interest.

References

1. Holechek, J.L.; Geli, H.M.E.; Sawalhah, M.N.; Valdez, R. A Global Assessment: Can Renewable Energy Replace Fossil Fuels by 2050? *Sustainability* **2022**, *14*, 4792. [[CrossRef](#)]
2. Intergovernmental Panel on Climate Change (IPCC). “Climate Change 2021—The Physical Science Basis: Working Group I Contribution to the Sixth Assessment Report of the Intergovernmental Panel on Climate Change”, Climate Change 2021—The Physical Science Basis. July 2023. Available online: <https://www.cambridge.org/core/books/climate-change-2021-the-physical-science-basis/415F29233B8BD19FB55F65E3DC67272B> (accessed on 22 January 2024).
3. “Greenhouse Gas Concentrations—Canada.ca”. Available online: <https://www.canada.ca/en/environment-climate-change/services/environmental-indicators/greenhouse-gas-concentrations.html> (accessed on 31 January 2024).
4. COP28 UAE. Available online: <https://www.cop28.com/en/> (accessed on 8 April 2024).

5. Sakunai, T.; Ito, L.; Tokai, A. Environmental impact assessment on production and material supply stages of lithium-ion batteries with increasing demands for electric vehicles. *J. Mater. Cycles Waste Manag.* **2021**, *23*, 470–479. [[CrossRef](#)]
6. Transport—Energy System—IEA. Available online: <https://www.iea.org/energy-system/transport> (accessed on 31 January 2024).
7. Liu, W.; Placke, T.; Chau, K.T. Overview of batteries and battery management for electric vehicles. *Energy Rep.* **2022**, *8*, 4058–4084. [[CrossRef](#)]
8. Global EV Data Explorer. Available online: <https://www.iea.org/data-and-statistics/data-tools/global-ev-data-explorer> (accessed on 14 May 2024).
9. Policy Developments—Global EV Outlook 2023—Analysis—IEA. Available online: <https://www.iea.org/reports/global-ev-outlook-2023/policy-developments> (accessed on 31 January 2024).
10. Shin, J.; Choi, J.W.; Shin, J.; Choi, J.W. Opportunities and Reality of Aqueous Rechargeable Batteries. *Adv. Energy Mater.* **2020**, *10*, 2001386. [[CrossRef](#)]
11. Zhang, L.; Wu, X.; Qian, W.; Pan, K.; Zhang, X.; Li, L.; Jia, M.; Zhang, S. Exploring More Functions in Binders for Lithium Batteries. *Electrochem. Energy Rev.* **2023**, *6*, 36. [[CrossRef](#)]
12. Chen, J.; Liu, J.; Qi, Y.; Sun, T.; Li, X. Unveiling the Roles of Binder in the Mechanical Integrity of Electrodes for Lithium-Ion Batteries. *J. Electrochem. Soc.* **2013**, *160*, A1502–A1509. [[CrossRef](#)]
13. Olabi, A.G.; Abbas, Q.; Shinde, P.A.; Abdelkareem, M.A. Rechargeable batteries: Technological advancement, challenges, current and emerging applications. *Energy* **2023**, *266*, 126408. [[CrossRef](#)]
14. Wang, Y.-B.; Yang, Q.; Guo, X.; Yang, S.; Chen, A.; Liang, G.-J.; Zhi, C.-Y. Strategies of binder design for high-performance lithium-ion batteries: A mini review. *Rare Met.* **2021**, *41*, 745–761. [[CrossRef](#)]
15. Nekahi, A.; MR, A.K.; Li, X.; Deng, S.; Zaghib, K. Sustainable LiFePO₄ and LiMnxFe1-xPO₄ (x = 0.1–1) cathode materials for lithium-ion batteries: A systematic review from mine to chassis. *Mater. Sci. Eng. R Rep.* **2024**, *159*, 100797. [[CrossRef](#)]
16. Goodenough, J.B.; Park, K.-S. The Li-Ion Rechargeable Battery: A Perspective. *J. Am. Chem. Soc.* **2013**, *135*, 1167–1176. [[CrossRef](#)]
17. Whittingham, M.S. Materials challenges facing electrical energy storage. *MRS Bull.* **2008**, *33*, 411–419. [[CrossRef](#)]
18. Hwang, J.-Y.; Myung, S.-T.; Sun, Y.-K. Sodium-ion batteries: Present and future. *Chem. Soc. Rev.* **2017**, *46*, 3529–3614. [[CrossRef](#)] [[PubMed](#)]
19. Chen, R.; Li, Q.; Yu, X.; Chen, L.; Li, H. Approaching Practically Accessible Solid-State Batteries: Stability Issues Related to Solid Electrolytes and Interfaces. *Chem. Rev.* **2020**, *120*, 6820–6877. [[CrossRef](#)] [[PubMed](#)]
20. Lingappan, N.; Kong, L.; Pecht, M. The significance of aqueous binders in lithium-ion batteries. *Renew. Sustain. Energy Rev.* **2021**, *147*, 111227. [[CrossRef](#)]
21. Nzereogu, P.U.; Omah, A.D.; Ezema, F.I.; Iwuoha, E.I.; Nwanya, A.C. Anode materials for lithium-ion batteries: A review. *Appl. Surf. Sci. Adv.* **2022**, *9*, 100233. [[CrossRef](#)]
22. Cheng, H.; Shapter, J.G.; Li, Y.; Gao, G. Recent progress of advanced anode materials of lithium-ion batteries. *J. Energy Chem.* **2021**, *57*, 451–468. [[CrossRef](#)]
23. Mohamed, N.; Allam, N.K. Recent advances in the design of cathode materials for Li-ion batteries. *RSC Adv.* **2020**, *10*, 21662–21685. [[CrossRef](#)] [[PubMed](#)]
24. Lee, W.; Muhammad, S.; Chernov, S.; Lee, H.; Yoon, J.; Kang, Y.-M.; Yoon, W.-S. Advances in the Cathode Materials for Lithium Rechargeable Batteries. *Angew. Chem. Int. Ed.* **2020**, *59*, 2578–2605. [[CrossRef](#)]
25. Jamesh, M.I.; Prakash, A.S. Advancement of technology towards developing Na-ion batteries. *J. Power Sources* **2018**, *378*, 268–300. [[CrossRef](#)]
26. Thakur, A.K.; Ahmed, M.S.; Oh, G.; Kang, H.; Jeong, Y.; Prabakaran, R.; Vikram, M.P.; Sharshir, S.W.; Kim, J.; Hwang, J.-Y. Advancement in graphene-based nanocomposites as high capacity anode materials for sodium-ion batteries. *J. Mater. Chem. A* **2021**, *9*, 2628–2661. [[CrossRef](#)]
27. Chen, H.; Ling, M.; Hencz, L.; Ling, H.Y.; Li, G.; Lin, Z.; Liu, G.; Zhang, S. Exploring Chemical, Mechanical, and Electrical Functionalities of Binders for Advanced Energy-Storage Devices. *Chem. Rev.* **2018**, *118*, 8936–8982. [[CrossRef](#)] [[PubMed](#)]
28. Jeschull, F.; Maibach, J.; Edström, K.; Brandell, D. On the Electrochemical Properties and Interphase Composition of Graphite: PVdF-HFP Electrodes in Dependence of Binder Content. *J. Electrochem. Soc.* **2017**, *164*, A1765–A1772. [[CrossRef](#)]
29. Ma, Y.; Ma, J.; Cui, G. Small things make big deal: Powerful binders of lithium batteries and post-lithium batteries. *Energy Storage Mater.* **2019**, *20*, 146–175. [[CrossRef](#)]
30. Saal, A.; Hagemann, T.; Schubert, U.S. Polymers for Battery Applications—Active Materials, Membranes, and Binders. *Adv. Energy Mater.* **2021**, *11*, 2001984. [[CrossRef](#)]
31. Ohashi, K.; Miyaki, Y.; Goto, K. Binders for Electrodes and Their Production Method. WO1997032347A1, 4 September 1997.
32. Whittingham, M.S. Electrical Energy Storage and Intercalation Chemistry. *Science* **1976**, *192*, 1126–1127. [[CrossRef](#)] [[PubMed](#)]
33. Whittingham, M.S. Lithium batteries and cathode materials. *Chem. Rev.* **2004**, *104*, 4271–4301. [[CrossRef](#)] [[PubMed](#)]
34. Whittingham, M.S. Chemistry of intercalation compounds: Metal guests in chalcogenide hosts. *Prog. Solid State Chem.* **1978**, *12*, 41–99. [[CrossRef](#)]
35. Armand, M.B.; Whittingham, M.S.; Huggins, R.A. The iron cyanide bronzes. *Mater. Res. Bull.* **1972**, *7*, 101–107. [[CrossRef](#)]
36. Mizushima, K.; Jones, P.C.; Wiseman, P.J.; Goodenough, J.B. Li_xCoO₂ (0 < x < 1): A new cathode material for batteries of high energy density. *Mater. Res. Bull.* **1980**, *15*, 783–789.

37. Liu, Q.; Su, X.; Lei, D.; Qin, Y.; Wen, J.; Guo, F.; Wu, Y.A.; Rong, Y.; Kou, R.; Xiao, X.; et al. Approaching the capacity limit of lithium cobalt oxide in lithium ion batteries via lanthanum and aluminium doping. *Nat. Energy* **2018**, *3*, 936–943. [CrossRef]
38. Xie, J.; Lu, Y.C. A retrospective on lithium-ion batteries. *Nat. Commun.* **2020**, *11*, 2499. [CrossRef] [PubMed]
39. Akira, Y.; Kenichi, S.; Takayuki, N. Secondary battery. US4668595A, 26 May 1987.
40. Placke, T.; Kloepsch, R.; Dühnen, S.; Winter, M. Lithium ion, lithium metal, and alternative rechargeable battery technologies: The odyssey for high energy density. *J. Solid State Electrochem.* **2017**, *21*, 1939–1964. [CrossRef]
41. Ozawa, K. Lithium-ion rechargeable batteries with LiCoO₂ and carbon electrodes: The LiCoO₂/C system. *Solid State Ion* **1994**, *69*, 212–221. [CrossRef]
42. Megahed, S.; Scrosati, B. Lithium-ion rechargeable batteries. *J. Power Sources* **1994**, *51*, 79–104. [CrossRef]
43. Adelhelm, P.; Hartmann, P.; Bender, C.L.; Busche, M.; Eufinger, C.; Janek, J. From lithium to sodium: Cell chemistry of room temperature sodium-air and sodium-sulfur batteries. *Beilstein J. Nanotechnol.* **2015**, *6*, 1016–1055. [CrossRef] [PubMed]
44. Newman, G.H.; Klemann, L.P. Ambient Temperature Cycling of an Na-TiS₂ Cell. *J. Electrochem. Soc.* **1980**, *127*, 2097–2099. [CrossRef]
45. Delmas, C.; Braconnier, J.; Fouassier, C.; Hagenmuller, P. Electrochemical intercalation of sodium in Na_xCoO₂ bronzes. *Solid State Ion* **1981**, *3–4*, 165–169. [CrossRef]
46. Yabuuchi, N.; Kubota, K.; Dahbi, M.; Komaba, S. Research Development on Sodium-Ion Batteries. *Chem. Rev.* **2014**, *114*, 11636–11682. [CrossRef] [PubMed]
47. Okada, S.; Takahashi, Y.; Kiyabu, T.; Doi, T.; Yamaki, J.-I.; Nishida, T. Layered Transition Metal Oxides as Cathodes for Sodium Secondary Battery. *ECS Meet. Abstr.* **2006**, MA2006-02, 201. [CrossRef]
48. Li, J.-T.; Wu, Z.-Y.; Lu, Y.-Q.; Zhou, Y.; Huang, Q.-S.; Huang, L.; Sun, S.-G. Water Soluble Binder, an Electrochemical Performance Booster for Electrode Materials with High Energy Density. *Adv. Energy Mater.* **2017**, *7*, 1701185. [CrossRef]
49. Kraytsberg, A.; Ein-Eli, Y. Higher, Stronger, Better... A Review of 5 Volt Cathode Materials for Advanced Lithium-Ion Batteries. *Adv. Energy Mater.* **2012**, *2*, 922–939. [CrossRef]
50. Kang, G.; Cao, Y. Application and modification of poly(vinylidene fluoride) (PVDF) membranes—A review. *J. Memb. Sci.* **2014**, *463*, 145–165. [CrossRef]
51. Zhang, Z.; Zeng, T.; Lai, Y.; Jia, M.; Li, J. A comparative study of different binders and their effects on electrochemical properties of LiMn₂O₄ cathode in lithium ion batteries. *J. Power Sources* **2014**, *247*, 1–8. [CrossRef]
52. Marshall, J.E.; Zhenova, A.; Roberts, S.; Petchey, T.; Zhu, P.; Dancer, C.E.; McElroy, C.R.; Kendrick, E. On the Solubility and Stability of Polyvinylidene Fluoride. *Polymers* **2021**, *13*, 1354. [CrossRef] [PubMed]
53. Bai, Y.; Muralidharan, N.; Li, J.; Essehli, R.; Belharouak, I. Sustainable Direct Recycling of Lithium-Ion Batteries via Solvent Recovery of Electrode Materials. Available online: <http://energy.gov/downloads/doe-public-access-plan> (accessed on 22 March 2024).
54. Biensan, P.; Simon, B.; Peres, J.P.; De Guibert, A.; Broussely, M.; Bodet, J.M.; Perton, F. On safety of lithium-ion cells. *J. Power Sources* **1999**, *81–82*, 906–912. [CrossRef]
55. Lux, S.F.; Schappacher, F.; Balducci, A.; Passerini, S.; Winter, M. Low Cost, Environmentally Benign Binders for Lithium-Ion Batteries. *J. Electrochem. Soc.* **2010**, *157*, A320. [CrossRef]
56. Xu, J.; Chou, S.L.; Gu, Q.F.; Liu, H.K.; Dou, S.X. The effect of different binders on electrochemical properties of LiNi_{1/3}Mn_{1/3}Co_{1/3}O₂ cathode material in lithium ion batteries. *J. Power Sources* **2013**, *225*, 172–178. [CrossRef]
57. Lee, J.-H.; Paik, U.; Hackley, V.A.; Choi, Y.-M. Effect of Carboxymethyl Cellulose on Aqueous Processing of Natural Graphite Negative Electrodes and their Electrochemical Performance for Lithium Batteries. *J. Electrochem. Soc.* **2005**, *152*, A1763. [CrossRef]
58. Bouguern, M.D.; Reddy, A.K.M.R.; Li, X.; Deng, S.; Laryea, H.; Zaghib, K. Engineering Dry Electrode Manufacturing for Sustainable Lithium-Ion Batteries. *Batteries* **2024**, *10*, 39. [CrossRef]
59. Bai, Y.; Hawley, W.B.; Jafta, C.J.; Muralidharan, N.; Polzin, B.J.; Belharouak, I. Sustainable recycling of cathode scraps via Cyrene-based separation. *Sustain. Mater. Technol.* **2020**, *25*, e00202. [CrossRef]
60. Clarke, C.J.; Tu, W.-C.; Levers, O.; Bröhl, A.; Hallett, J.P. Green and Sustainable Solvents in Chemical Processes. *Chem. Rev.* **2018**, *118*, 747–800. [CrossRef] [PubMed]
61. Luo, L.; Xu, Y.; Zhang, H.; Han, X.; Dong, H.; Xu, X.; Chen, C.; Zhang, Y.; Lin, J. Comprehensive Understanding of High Polar Polyacrylonitrile as an Effective Binder for Li-Ion Battery Nano-Si Anodes. *ACS Appl. Mater. Interfaces* **2016**, *8*, 8154–8161. [CrossRef]
62. Dou, W.; Zheng, M.; Zhang, W.; Liu, T.; Wang, F.; Wan, G.; Liu, Y.; Tao, X. Review on the Binders for Sustainable High-Energy-Density Lithium Ion Batteries: Status, Solutions, and Prospects. *Adv. Funct. Mater.* **2023**, *33*, 2305161. [CrossRef]
63. Tron, A.; Park, Y.D.; Mun, J. AlF₃-coated LiMn₂O₄ as cathode material for aqueous rechargeable lithium battery with improved cycling stability. *J. Power Sources* **2016**, *325*, 360–364. [CrossRef]
64. Zhang, Z.; Zeng, T.; Qu, C.; Lu, H.; Jia, M.; Lai, Y.; Li, J. Cycle performance improvement of LiFePO₄ cathode with polyacrylic acid as binder. *Electrochim. Acta* **2012**, *80*, 440–444. [CrossRef]
65. Zhang, S.S.; Xu, K.; Jow, T.R. Evaluation on a water-based binder for the graphite anode of Li-ion batteries. *J. Power Sources* **2004**, *138*, 226–231. [CrossRef]

66. Yen, J.-P.; Chang, C.-C.; Lin, Y.-R.; Shen, S.-T.; Hong, J.-L. Effects of Styrene-Butadiene Rubber/Carboxymethylcellulose (SBR/CMC) and Polyvinylidene Difluoride (PVDF) Binders on Low Temperature Lithium Ion Batteries. *J. Electrochem. Soc.* **2013**, *160*, A1811–A1818. [[CrossRef](#)]
67. Mazouzi, D.; Karkar, Z.; Hernandez, C.R.; Manero, P.J.; Guyomard, D.; Roué, L.; Lestriez, B. Critical roles of binders and formulation at multiscales of silicon-based composite electrodes. *J. Power Sources* **2015**, *280*, 533–549. [[CrossRef](#)]
68. Chen, Z.; Christensen, L.; Dahn, J.R. Large-volume-change electrodes for Li-ion batteries of amorphous alloy particles held by elastomeric tethers. *Electrochem. Commun.* **2003**, *5*, 919–923. [[CrossRef](#)]
69. Vogt, L.O.; El Kazzi, M.; Berg, E.J.; Villar, S.P.; Novák, P.; Villevieille, C. Understanding the Interaction of the Carbonates and Binder in Na-Ion Batteries: A Combined Bulk and Surface Study. *Chem. Mater.* **2015**, *27*, 1210–1216. [[CrossRef](#)]
70. Ostrovskii, D.; Jacobsson, P. Concentrational changes in PAN-based polymer gel electrolyte under current flow: In situ micro-Raman investigation. *J. Power Sources* **2001**, *97*–*98*, 667–670. [[CrossRef](#)]
71. Peramunage, D.; Pasquariello, D.M.; Abraham, K.M. Polyacrylonitrile-Based Electrolytes with Ternary Solvent Mixtures as Plasticizers. *J. Electrochem. Soc.* **1995**, *142*, 1789–1798. [[CrossRef](#)]
72. Mindemark, J.; Lacey, M.J.; Bowden, T.; Brandell, D. Beyond PEO—Alternative host materials for Li⁺-conducting solid polymer electrolytes. *Prog. Polym. Sci.* **2018**, *81*, 114–143. [[CrossRef](#)]
73. Gong, L.; Nguyen, M.H.T.; Oh, E.-S. High polar polyacrylonitrile as a potential binder for negative electrodes in lithium ion batteries. *Electrochem. Commun.* **2013**, *29*, 45–47. [[CrossRef](#)]
74. Kim, E.-Y.; Lee, B.-R.; Yun, G.; Oh, E.-S.; Lee, H. Effects of binder content on manganese dissolution and electrochemical performances of spinel lithium manganese oxide cathodes for lithium ion batteries. *Curr. Appl. Phys.* **2015**, *15*, 429–434. [[CrossRef](#)]
75. Li, G.; Liao, Y.; He, Z.; Zhou, H.; Xu, N.; Lu, Y.; Sun, G.; Li, W. A new strategy to improve the cyclic stability of high voltage lithium nickel manganese oxide cathode by poly(butyl methacrylate-acrylonitrile-styrene) terpolymer as co-binder in lithium ion batteries. *Electrochim. Acta* **2019**, *319*, 527–540. [[CrossRef](#)]
76. Yang, X.; Shen, L.; Wu, B.; Zuo, Z.; Mu, D.; Wu, B.; Zhou, H. Improvement of the cycling performance of LiCoO₂ with assistance of cross-linked PAN for lithium ion batteries. *J. Alloys Compd.* **2015**, *639*, 458–464. [[CrossRef](#)]
77. Tsao, C.-H.; Hsu, C.-H.; Kuo, P.-L. Ionic Conducting and Surface Active Binder of Poly(ethylene oxide)-block-poly(acrylonitrile) for High Power Lithium-ion Battery. *Electrochim. Acta* **2016**, *196*, 41–47. [[CrossRef](#)]
78. Chen, Y.; Liu, S.; Cheng, S.; Gao, S.; Chai, J.; Jiang, Q.; Liu, Z.; Liu, X.; Liu, J.; Xie, M.; et al. Insight into Superior Electrochemical Performance of 4.5 V High-Voltage LiCoO₂ Using a Robust Polyacrylonitrile Binder. *ACS Appl. Energy Mater.* **2022**, *5*, 3072–3080. [[CrossRef](#)]
79. Umirov, N.; Moon, S.; Park, G.; Kim, H.-Y.; Lee, K.J.; Kim, S.-S. Novel silane-treated polyacrylonitrile as a promising negative electrode binder for LIBs. *J. Alloys Compd.* **2020**, *815*, 152481. [[CrossRef](#)]
80. Jin, J.; Yu, B.; Shi, Z.; Wang, C.; Chong, C. Lignin-based electrospun carbon nanofibrous webs as free-standing and binder-free electrodes for sodium ion batteries. *J. Power Sources* **2014**, *272*, 800–807. [[CrossRef](#)]
81. Campéon, B.D.L.; Umezawa, R.; Pandey, A.K.; Ishikawa, T.; Tsuchiya, Y.; Ishigaki, Y.; Kanto, R.; Yabuuchi, N. Efficient Surface Passivation of Ti-Based Layered Materials by a Nonfluorine Branched Copolymer for Durable and High-Power Sodium-Ion Batteries. *ACS Appl. Mater. Interfaces* **2024**, *16*, 3396–3405. [[CrossRef](#)] [[PubMed](#)]
82. Bresser, D.; Buchholz, D.; Moretti, A.; Varzi, A.; Passerini, S. Alternative binders for sustainable electrochemical energy storage—The transition to aqueous electrode processing and bio-derived polymers. *Energy Environ. Sci.* **2018**, *11*, 3096–3127. [[CrossRef](#)]
83. Priyono, S.; Lubis, B.M.; Humaidi, S.; Prihandoko, B. Heating Effect on Manufacturing Li₄Ti₅O₁₂ Electrode Sheet with PTFE Binder on Battery Cell Performance. *IOP Conf. Ser. Mater. Sci. Eng.* **2018**, *367*, 012007. [[CrossRef](#)]
84. Zhang, X.; Ge, X.; Shen, Z.; Ma, H.; Wang, J.; Wang, S.; Liu, L.; Liu, B.; Liu, L.; Zhao, Y. Green water-based binders for LiFePO₄/C cathodes in Li-ion batteries: A comparative study. *New J. Chem.* **2021**, *45*, 9846–9855. [[CrossRef](#)]
85. Rae, P.J.; Brown, E.N. The properties of poly(tetrafluoroethylene) (PTFE) in tension. *Polymer (Guildf)* **2005**, *46*, 8128–8140. [[CrossRef](#)]
86. Pruitt, L.A. Deformation, yielding, fracture and fatigue behavior of conventional and highly cross-linked ultra high molecular weight polyethylene. *Biomaterials* **2005**, *26*, 905–915. [[CrossRef](#)] [[PubMed](#)]
87. Li, W.; Mays, S.; Lam, D. Material and finite element analysis of poly(tetrafluoroethylene) rotary seals. *Plast. Rubber Compos.* **2002**, *31*, 359–363. [[CrossRef](#)]
88. Brown, E.N.; Rae, P.J.; Orler, E.B.; Gray, G.T.; Dattelbaum, D.M. The effect of crystallinity on the fracture of polytetrafluoroethylene (PTFE). *Mater. Sci. Eng. C* **2006**, *26*, 1338–1343. [[CrossRef](#)]
89. Brown, E.N.; Dattelbaum, D.M. The role of crystalline phase on fracture and microstructure evolution of polytetrafluoroethylene (PTFE). *Polymer (Guildf)* **2005**, *46*, 3056–3068. [[CrossRef](#)]
90. Joyce, J.A. Fracture toughness evaluation of polytetrafluoroethylene. *Polym. Eng. Sci.* **2003**, *43*, 1702–1714. [[CrossRef](#)]
91. Wang, X.; Chen, S.; Zhang, K.; Huang, L.; Shen, H.; Chen, Z.; Rong, C.; Wang, G.; Jiang, Z. A Polytetrafluoroethylene-Based Solvent-Free Procedure for the Manufacturing of Lithium-Ion Batteries. *Materials* **2023**, *16*, 7232. [[CrossRef](#)]
92. Gao, S.; Su, Y.; Bao, L.; Li, N.; Chen, L.; Zheng, Y.; Tian, J.; Li, J.; Chen, S.; Wu, F. High-performance LiFePO₄/C electrode with polytetrafluoroethylene as an aqueous-based binder. *J. Power Sources* **2015**, *298*, 292–298. [[CrossRef](#)]
93. Sisanth, K.S.; Thomas, M.G.; Abraham, J.; Thomas, S. General introduction to rubber compounding. In *Progress in Rubber Nanocomposites*; Elsevier: Amsterdam, The Netherlands, 2017; pp. 1–39. [[CrossRef](#)]

94. Yoshio, M.; Kugino, S.; Dimov, N. Electrochemical behaviors of silicon based anode material. *J. Power Sources* **2006**, *153*, 375–379. [[CrossRef](#)]
95. Buqa, H.; Holzapfel, M.; Krumeich, F.; Veit, C.; Novák, P. Study of styrene butadiene rubber and sodium methyl cellulose as binder for negative electrodes in lithium-ion batteries. *J. Power Sources* **2006**, *161*, 617–622. [[CrossRef](#)]
96. Zhang, R.; Yang, X.; Zhang, D.; Qiu, H.; Fu, Q.; Na, H.; Guo, Z.; Du, F.; Chen, G.; Wei, Y. Water soluble styrene butadiene rubber and sodium carboxyl methyl cellulose binder for ZnFe₂O₄ anode electrodes in lithium ion batteries. *J. Power Sources* **2015**, *285*, 227–234. [[CrossRef](#)]
97. Li, J.; Le, D.-B.; Ferguson, P.P.; Dahn, J.R. Lithium polyacrylate as a binder for tin–cobalt–carbon negative electrodes in lithium-ion batteries. *Electrochim. Acta* **2010**, *55*, 2991–2995. [[CrossRef](#)]
98. Park, K.; Yoo, H.E.; Jung, Y.; Ryu, M.; Myeong, S.; Lee, D.; Kim, S.C.; Kim, C.; Kim, J.; Kwon, J.; et al. Styrene-butadiene rubber patterned current collector for improved Li-ion kinetics of the anode for high energy density lithium-ion batteries. *J. Power Sources* **2023**, *577*, 233238. [[CrossRef](#)]
99. Eom, J.-Y.; Kim, S.-I.; Ri, V.; Kim, C. The effect of polymeric binders in the sulfur cathode on the cycling performance for lithium–sulfur batteries. *Chem. Commun.* **2019**, *55*, 14609–14612. [[CrossRef](#)]
100. Zhao, Y.-M.; Yue, F.-S.; Li, S.-C.; Zhang, Y.; Tian, Z.-R.; Xu, Q.; Xin, S.; Guo, Y.-G. Advances of polymer binders for silicon-based anodes in high energy density lithium-ion batteries. *InfoMat* **2021**, *3*, 460–501. [[CrossRef](#)]
101. Zhang, Y.; Grant, A.; Carroll, A.; Gulzar, U.; Ferguson, M.; Roy, A.; Nicolosi, V.; O'Dwyer, C. Water-Soluble Binders That Improve Electrochemical Sodium-Ion Storage Properties in a NaTi₂(PO₄)₃ Anode. *J. Electrochem. Soc.* **2023**, *170*, 050529. [[CrossRef](#)]
102. Isozumi, H.; Horiba, T.; Kubota, K.; Hida, K.; Matsuyama, T.; Yasuno, S.; Komaba, S. Application of modified styrene-butadiene-rubber-based latex binder to high-voltage operating LiCoO₂ composite electrodes for lithium-ion batteries. *J. Power Sources* **2020**, *468*, 228332. [[CrossRef](#)]
103. Jolley, M.J.; Pathan, T.S.; Jenkins, C.; Loveridge, M.J. Investigating the effect of the degree of cross-linking in styrene butadiene rubber on the performance of graphite anodes for the use in lithium-ion batteries. *J. Appl. Polym. Sci.* **2024**, *141*, e55135. [[CrossRef](#)]
104. Ma, Z.; Lyu, Y.; Yang, H.; Li, Q.; Guo, B.; Nie, A. Systematic investigation of the Binder's role in the electrochemical performance of tin sulfide electrodes in SIBs. *J. Power Sources* **2018**, *401*, 195–203. [[CrossRef](#)]
105. Parikh, P.; Sina, M.; Banerjee, A.; Wang, X.; D'Souza, M.S.; Doux, J.M.; Wu, E.A.; Trieu, O.Y.; Gong, Y.; Zhou, Q.; et al. Role of Polyacrylic Acid (PAA) Binder on the Solid Electrolyte Interphase in Silicon Anodes. *Chem. Mater.* **2019**, *31*, 2535–2544. [[CrossRef](#)]
106. Fan, Q.; Zhang, W.; Duan, J.; Hong, K.; Xue, L.; Huang, Y. Effects of binders on electrochemical performance of nitrogen-doped carbon nanotube anode in sodium-ion battery. *Electrochim. Acta* **2015**, *174*, 970–977. [[CrossRef](#)]
107. Fan, X.; Hsieh, Y.; Krochta, J.M.; Kurth, M.J. Study on molecular interaction behavior, and thermal and mechanical properties of polyacrylic acid and lactose blends. *J. Appl. Polym. Sci.* **2001**, *82*, 1921–1927. [[CrossRef](#)]
108. Hu, B.; Shkrob, I.A.; Zhang, S.; Zhang, L.; Zhang, J.; Li, Y.; Liao, C.; Zhang, Z.; Lu, W.; Zhang, L. The existence of optimal molecular weight for poly(acrylic acid) binders in silicon/graphite composite anode for lithium-ion batteries. *J. Power Sources* **2018**, *378*, 671–676. [[CrossRef](#)]
109. Sun, F.; Wheeler, D.R. The Effects of Lithium Ions and pH on the Function of Polyacrylic Acid Binder for Silicon Anodes. *J. Electrochem. Soc.* **2023**, *170*, 080502. [[CrossRef](#)]
110. Magasinski, A.; Zdyrko, B.; Kovalenko, I.; Hertzberg, B.; Burtovyy, R.; Huebner, C.F.; Fuller, T.F.; Luzinov, I.; Yushin, G. Toward Efficient Binders for Li-Ion Battery Si-Based Anodes: Polyacrylic Acid. *ACS Appl. Mater. Interfaces* **2010**, *2*, 3004–3010. [[CrossRef](#)]
111. Ui, K.; Kikuchi, S.; Mikami, F.; Kadoma, Y.; Kumagai, N. Improvement of electrochemical characteristics of natural graphite negative electrode coated with polyacrylic acid in pure propylene carbonate electrolyte. *J. Power Sources* **2007**, *173*, 518–521. [[CrossRef](#)]
112. Nguyen, V.H.; Wang, W.L.; Jin, E.M.; Gu, H.-B. Impacts of different polymer binders on electrochemical properties of LiFePO₄ cathode. *Appl. Surf. Sci.* **2013**, *282*, 444–449. [[CrossRef](#)]
113. Cai, Z.P.; Liang, Y.; Li, W.S.; Xing, L.D.; Liao, Y.H. Preparation and performances of LiFePO₄ cathode in aqueous solvent with polyacrylic acid as a binder. *J. Power Sources* **2009**, *189*, 547–551. [[CrossRef](#)]
114. Mathew, A.; van Ekeren, W.; Andersson, R.; Lacey, M.J.; Heiskanen, S.K.; Younesi, R.; Brandell, D. Limitations of Polyacrylic Acid Binders When Employed in Thick LNMO Li-ion Battery Electrodes. *J. Electrochem. Soc.* **2024**, *171*, 020531. [[CrossRef](#)]
115. Nagulapati, V.M.; Kim, D.S.; Oh, J.; Lee, J.H.; Hur, J.; Kim, I.T.; Lee, S.G. Enhancing the Electrochemical Performance of SbTe Bimetallic Anodes for High-Performance Sodium-Ion Batteries: Roles of the Binder and Carbon Support Matrix. *Nanomaterials* **2019**, *9*, 1134. [[CrossRef](#)] [[PubMed](#)]
116. Chai, L.; Qu, Q.; Zhang, L.; Shen, M.; Zhang, L.; Zheng, H. Chitosan, a new and environmental benign electrode binder for use with graphite anode in lithium-ion batteries. *Electrochim. Acta* **2013**, *105*, 378–383. [[CrossRef](#)]
117. Hamzelui, N.; Linhorst, M.; Nyenhuis, G.M.; Haneke, L.; Eshetu, G.G.; Placke, T.; Winter, M.; Moerschbacher, B.M.; Figgemeier, E. Chitosan as Enabling Polymeric Binder Material for Silicon-Graphite-Based Anodes in Lithium-Ion Batteries. *Energy Technol.* **2023**, *11*, 2201239. [[CrossRef](#)]
118. Gopakumar, D.A.; Pai, A.R.; Pasquini, D.; Shao-Yuan, L.; HPS, A.K.; Thomas, S. Nanomaterials—State of Art, New Challenges, and Opportunities. In *Nanoscale Materials in Water Purification*; Elsevier: Amsterdam, The Netherlands, 2019; pp. 1–24. [[CrossRef](#)]
119. Cord-Landwehr, S.; Moerschbacher, B.M. Deciphering the ChitoCode: Fungal chitins and chitosans as functional biopolymers. *Fungal. Biol. Biotechnol.* **2021**, *8*, 19. [[CrossRef](#)]

120. Yue, L.; Zhang, L.; Zhong, H. Carboxymethyl chitosan: A new water soluble binder for Si anode of Li-ion batteries. *J. Power Sources* **2014**, *247*, 327–331. [[CrossRef](#)]
121. Shih, F.-Y.; Fung, K.-Z.; Wang, J.-W. Fabrication of LiMn_2O_4 thin film cathode from chitosan-containing solution. *J. Alloys Compd.* **2006**, *407*, 282–288. [[CrossRef](#)]
122. Prasanna, K.; Subburaj, T.; Jo, Y.N.; Lee, W.J.; Lee, C.W. Environment-Friendly Cathodes Using Biopolymer Chitosan with Enhanced Electrochemical Behavior for Use in Lithium Ion Batteries. *ACS Appl. Mater. Interfaces* **2015**, *7*, 7884–7890. [[CrossRef](#)] [[PubMed](#)]
123. Cui, J.; Yu, Z.; Lau, D. Effect of Acetyl Group on Mechanical Properties of Chitin/Chitosan Nanocrystal: A Molecular Dynamics Study. *Int. J. Mol. Sci.* **2016**, *17*, 61. [[CrossRef](#)] [[PubMed](#)]
124. Gao, H.; Zhou, W.; Jang, J.; Goodenough, J.B. Cross-Linked Chitosan as a Polymer Network Binder for an Antimony Anode in Sodium-Ion Batteries. *Adv. Energy Mater.* **2016**, *6*, 1502130. [[CrossRef](#)]
125. Russo, R.; Malinconico, M.; Santagata, G. Effect of Cross-Linking with Calcium Ions on the Physical Properties of Alginate Films. *Biomacromolecules* **2007**, *8*, 3193–3197. [[CrossRef](#)] [[PubMed](#)]
126. Smidsrød, O.; Skjakbrk, G. Alginate as immobilization matrix for cells. *Trends Biotechnol.* **1990**, *8*, 71–78. [[CrossRef](#)] [[PubMed](#)]
127. Yoon, J.; Oh, D.X.; Jo, C.; Lee, J.; Hwang, D.S. Improvement of desolvation and resilience of alginate binders for Si-based anodes in a lithium ion battery by calcium-mediated cross-linking. *Phys. Chem. Chem. Phys.* **2014**, *16*, 25628–25635. [[CrossRef](#)] [[PubMed](#)]
128. Song, J.; Zhou, M.; Yi, R.; Xu, T.; Gordin, M.L.; Tang, D.; Yu, Z.; Regula, M.; Wang, D. Interpenetrated Gel Polymer Binder for High-Performance Silicon Anodes in Lithium-ion Batteries. *Adv. Funct. Mater.* **2014**, *24*, 5904–5910. [[CrossRef](#)]
129. Deng, S.; Wang, H.; Liu, H.; Liu, J.; Yan, H. Research Progress in Improving the Rate Performance of LiFePO_4 Cathode Materials. *Nanomicro Lett.* **2014**, *6*, 209–226. [[CrossRef](#)]
130. Zhang, S.; Ren, S.; Han, D.; Xiao, M.; Wang, S.; Meng, Y. Aqueous sodium alginate as binder: Dramatically improving the performance of dilithium terephthalate-based organic lithium ion batteries. *J. Power Sources* **2019**, *438*, 227007. [[CrossRef](#)]
131. Li, J.; Zhao, Y.; Wang, N.; Ding, Y.; Guan, L. Enhanced performance of a MnO_2 -graphene sheet cathode for lithium ion batteries using sodium alginate as a binder. *J. Mater. Chem.* **2012**, *22*, 13002. [[CrossRef](#)]
132. Zhang, L.; Zhang, L.; Chai, L.; Xue, P.; Hao, W.; Zheng, H. A coordinatively cross-linked polymeric network as a functional binder for high-performance silicon submicro-particle anodes in lithium-ion batteries. *J. Mater. Chem. A* **2014**, *2*, 19036–19045. [[CrossRef](#)]
133. Liu, J.; Zhang, Q.; Wu, Z.Y.; Wu, J.H.; Li, J.T.; Huang, L.; Sun, S.G. A high-performance alginate hydrogel binder for the Si/C anode of a Li-ion battery. *Chem. Commun.* **2014**, *50*, 6386. [[CrossRef](#)] [[PubMed](#)]
134. Ryou, M.H.; Kim, J.; Lee, I.; Kim, S.; Jeong, Y.K.; Hong, S.; Ryu, J.H.; Kim, T.S.; Park, J.K.; Lee, H.; et al. Mussel-Inspired Adhesive Binders for High-Performance Silicon Nanoparticle Anodes in Lithium-Ion Batteries. *Adv. Mater.* **2013**, *25*, 1571–1576. [[CrossRef](#)] [[PubMed](#)]
135. Huang, H.; Chen, R.; Yang, S.; Zhang, W.; Fang, Y.; Li, L.; Liu, Y.; Huang, J. High-performance Si flexible anode with rGO substrate and Ca^{2+} crosslinked sodium alginate binder for lithium ion battery. *Synth. Met.* **2019**, *247*, 212–218. [[CrossRef](#)]
136. Ling, L.; Bai, Y.; Wang, Z.; Ni, Q.; Chen, G.; Zhou, Z.; Wu, C. Remarkable Effect of Sodium Alginate Aqueous Binder on Anatase TiO_2 as High-Performance Anode in Sodium Ion Batteries. *ACS Appl. Mater. Interfaces* **2018**, *10*, 5560–5568. [[CrossRef](#)] [[PubMed](#)]
137. Xu, H.; Jiang, K.; Zhang, X.; Zhang, X.; Guo, S.; Zhou, H. Sodium Alginate Enabled Advanced Layered Manganese-Based Cathode for Sodium-Ion Batteries. *ACS Appl. Mater. Interfaces* **2019**, *11*, 26817–26823. [[CrossRef](#)] [[PubMed](#)]
138. Le, T.-H.; Kim, Y.; Yoon, H. Electrical and Electrochemical Properties of Conducting Polymers. *Polymers* **2017**, *9*, 150. [[CrossRef](#)] [[PubMed](#)]
139. Nguyen, V.A.; Kuss, C. Review—Conducting Polymer-Based Binders for Lithium-Ion Batteries and Beyond. *J. Electrochem. Soc.* **2020**, *167*, 065501. [[CrossRef](#)]
140. Zhao, H.; Wang, Z.; Lu, P.; Jiang, M.; Shi, F.; Song, X.; Zheng, Z.; Zhou, X.; Fu, Y.; Abdelbast, G.; et al. Toward Practical Application of Functional Conductive Polymer Binder for a High-Energy Lithium-Ion Battery Design. *Nano Lett.* **2014**, *14*, 6704–6710. [[CrossRef](#)]
141. Kim, S.M.; Kim, M.H.; Choi, S.Y.; Lee, J.G.; Jang, J.; Lee, J.B.; Ryu, J.H.; Hwang, S.S.; Park, J.H.; Shin, K.; et al. Poly(phenanthrenequinone) as a conductive binder for nano-sized silicon negative electrodes. *Energy Environ. Sci.* **2015**, *8*, 1538–1543. [[CrossRef](#)]
142. Zheng, T.; Zhang, T.; de la Fuente, M.S.; Liu, G. Aqueous emulsion of conductive polymer binders for Si anode materials in lithium ion batteries. *Eur. Polym. J.* **2019**, *114*, 265–270. [[CrossRef](#)]
143. Higgins, T.M.; Park, S.H.; King, P.J.; Zhang, C.; McEvoy, N.; Berner, N.C.; Daly, D.; Shmeliov, A.; Khan, U.; Duesberg, G.; et al. A Commercial Conducting Polymer as Both Binder and Conductive Additive for Silicon Nanoparticle-Based Lithium-Ion Battery Negative Electrodes. *ACS Nano* **2016**, *10*, 3702–3713. [[CrossRef](#)] [[PubMed](#)]
144. Liu, D.; Zhao, Y.; Tan, R.; Tian, L.-L.; Liu, Y.; Chen, H.; Pan, F. Novel conductive binder for high-performance silicon anodes in lithium ion batteries. *Nano Energy* **2017**, *36*, 206–212. [[CrossRef](#)]
145. Yu, Y.; Zhu, J.; Li, Y.; Xu, Q.; Jiang, Y.; Yang, C.; Shi, L.; Chen, L.; Liu, P.; Zhang, J.; et al. Mixed ion-electron conductive binders coupling superior stiffness and toughness establish dual crosslinking stable silicon anodes. *Chem. Eng. J.* **2024**, *479*, 147807. [[CrossRef](#)]
146. Zhao, H.; Du, A.; Ling, M.; Battaglia, V.; Liu, G. Conductive polymer binder for nano-silicon/graphite composite electrode in lithium-ion batteries towards a practical application. *Electrochim. Acta* **2016**, *209*, 159–162. [[CrossRef](#)]

147. Lyness, C. Lithium-secondary cell: Sources of risks and their effects. In *Electrochemical Power Sources: Fundamentals, Systems, and Applications Li-Battery Safety*; Elsevier: Amsterdam, The Netherlands, 2018; pp. 143–266. [[CrossRef](#)]
148. Liu, Y.; Qian, K.; He, J.; Chu, X.; He, Y.-B.; Wu, M.; Li, B.; Kang, F. In-situ polymerized lithium polyacrylate (PAALi) as dual-functional lithium source for high-performance layered oxide cathodes. *Electrochim. Acta* **2017**, *249*, 43–51. [[CrossRef](#)]
149. Virya, A.; Lian, K. Lithium polyacrylate-polyacrylamide blend as polymer electrolytes for solid-state electrochemical capacitors. *Electrochim. Commun.* **2018**, *97*, 77–81. [[CrossRef](#)]
150. Rao, L.; Jiao, X.; Yu, C.-Y.; Schmidt, A.; O'Meara, C.; Seidt, J.; Sayre, J.R.; Khalifa, Y.M.; Kim, J.-H. Multifunctional Composite Binder for Thick High-Voltage Cathodes in Lithium-Ion Batteries. *ACS Appl. Mater. Interfaces* **2022**, *14*, 861–872. [[CrossRef](#)]
151. Zhong, H.; Lu, J.; He, A.; Sun, M.; He, J.; Zhang, L. Carboxymethyl chitosan/poly(ethylene oxide) water soluble binder: Challenging application for 5 V $\text{LiNi}_{0.5}\text{Mn}_{1.5}\text{O}_4$ cathode. *J. Mater. Sci. Technol.* **2017**, *33*, 763–767. [[CrossRef](#)]
152. Fu, Z.; Feng, H.L.; Xiang, X.D.; Rao, M.M.; Wu, W.; Luo, J.C.; Chen, T.T.; Hu, Q.P.; Feng, A.B.; Li, W.S. A novel polymer composite as cathode binder of lithium ion batteries with improved rate capability and cyclic stability. *J. Power Sources* **2014**, *261*, 170–174. [[CrossRef](#)]
153. Hapuarachchi, S.N.S.; Wasalathilake, K.C.; Nerkar, J.Y.; Jaatinen, E.; O'Mullane, A.P.; Yan, C. Mechanically Robust Tapioca Starch Composite Binder with Improved Ionic Conductivity for Sustainable Lithium-Ion Batteries. *ACS Sustain. Chem. Eng.* **2020**, *8*, 9857–9865. [[CrossRef](#)]
154. Shao, D.; Zhong, H.; Zhang, L. Water-Soluble Conductive Composite Binder Containing PEDOT:PSS as Conduction Promoting Agent for Si Anode of Lithium-Ion Batteries. *ChemElectroChem* **2014**, *1*, 1679–1687. [[CrossRef](#)]
155. Zhong, H.; He, A.; Lu, J.; Sun, M.; He, J.; Zhang, L. Carboxymethyl chitosan/conducting polymer as water-soluble composite binder for LiFePO_4 cathode in lithium ion batteries. *J. Power Sources* **2016**, *336*, 107–114. [[CrossRef](#)]
156. Kim, D.; Hwang, C.; Jeong, J.; Song, W.-J.; Park, S.; Song, H.-K. Bipolymer-Cross-Linked Binder to Improve the Reversibility and Kinetics of Sodiation and Desodiation of Antimony for Sodium-Ion Batteries. *ACS Appl. Mater. Interfaces* **2019**, *11*, 43039–43045. [[CrossRef](#)] [[PubMed](#)]
157. Wu, S.; Di, F.; Zheng, J.G.; Zhao, H.W.; Zhang, H.; Li, L.X.; Geng, X.; Sun, C.G.; Yang, H.M.; Zhou, W.M.; et al. Self-healing polymer binders for the Si and Si/carbon anodes of lithium-ion batteries. *New Carbon Mater.* **2022**, *37*, 802–826. [[CrossRef](#)]
158. Wang, S.; Urban, M.W. Self-healing polymers. *Nat. Rev. Mater.* **2020**, *5*, 562–583. [[CrossRef](#)]
159. Zhou, Y.; Li, L.; Han, Z.; Li, Q.; He, J.; Wang, Q. Self-Healing Polymers for Electronics and Energy Devices. *Chem. Rev.* **2023**, *123*, 558–612. [[CrossRef](#)]
160. Utrera-Barrios, S.; Verdejo, R.; López-Manchado, M.A.; Santana, M.H. Evolution of self-healing elastomers, from extrinsic to combined intrinsic mechanisms: A review. *Mater. Horiz.* **2020**, *7*, 2882–2902. [[CrossRef](#)]
161. Lim, T.; Yoon, J.; Lee, C.; Baek, K.-Y.; Jeon, J.-W.; Cho, S. Self-Healable and Degradable Polycaprolactone-Based Polymeric Binders for Lithium-Ion Batteries. *ACS Appl. Polym. Mater.* **2024**, *6*, 4050–4059. [[CrossRef](#)]
162. Yang, Y.; Urban, M.W. Self-Healing of Polymers via Supramolecular Chemistry. *Adv. Mater. Interfaces* **2018**, *5*, 1800384. [[CrossRef](#)]
163. Chen, L.; Wang, S.; Guo, Z.; Hu, Y. Double dynamic bonds tough hydrogel with high self-healing properties based on acylhydrazone bonds and borate bonds. *Polym. Adv. Technol.* **2022**, *33*, 2528–2541. [[CrossRef](#)]
164. Li, J.; Wang, Y.; Xie, X.; Kong, Z.; Tong, Y.; Xu, H.; Xu, H.; Jin, H. A novel multi-functional binder based on double dynamic bonds for silicon anode of lithium-ion batteries. *Electrochim. Acta* **2022**, *425*, 140620. [[CrossRef](#)]
165. Chen, Y.; Tang, Z.; Zhang, X.; Liu, Y.; Wu, S.; Guo, B. Covalently Cross-Linked Elastomers with Self-Healing and Malleable Abilities Enabled by Boronic Ester Bonds. *ACS Appl. Mater. Interfaces* **2018**, *10*, 24224–24231. [[CrossRef](#)]
166. Taynton, P.; Ni, H.; Zhu, C.; Yu, K.; Loob, S.; Jin, Y.; Qi, H.J.; Zhang, W. Repairable Woven Carbon Fiber Composites with Full Recyclability Enabled by Malleable Polyimine Networks. *Adv. Mater.* **2016**, *28*, 2904–2909. [[CrossRef](#)] [[PubMed](#)]
167. Zhang, X.; Chen, P.; Zhao, Y.; Liu, M.; Xiao, Z. High-Performance Self-Healing Polyurethane Binder Based on Aromatic Disulfide Bonds and Hydrogen Bonds for the Sulfur Cathode of Lithium–Sulfur Batteries. *Ind. Eng. Chem. Res.* **2021**, *60*, 12011–12020. [[CrossRef](#)]
168. Kwon, T.; Jeong, Y.K.; Lee, I.; Kim, T.; Choi, J.W.; Coskun, A. Systematic Molecular-Level Design of Binders Incorporating Meldrum's Acid for Silicon Anodes in Lithium Rechargeable Batteries. *Adv. Mater.* **2014**, *26*, 7979–7985. [[CrossRef](#)]
169. Kuo, T.-C.; Chiou, C.-Y.; Li, C.-C.; Lee, J.-T. In situ cross-linked poly(ether urethane) elastomer as a binder for high-performance Si anodes of lithium-ion batteries. *Electrochim. Acta* **2019**, *327*, 135011. [[CrossRef](#)]
170. Jeong, Y.K.; Kwon, T.; Lee, I.; Kim, T.-S.; Coskun, A.; Choi, J.W. Millipede-inspired structural design principle for high performance polysaccharide binders in silicon anodes. *Energy Environ. Sci.* **2015**, *8*, 1224–1230. [[CrossRef](#)]
171. Kim, J.; Choi, J.; Park, K.; Kim, S.; Nam, K.W.; Char, K.; Choi, J.W. Host–Guest Interlocked Complex Binder for Silicon–Graphite Composite Electrodes in Lithium Ion Batteries. *Adv. Energy Mater.* **2022**, *12*, 2103718. [[CrossRef](#)]
172. Kim, J.; Park, K.; Cho, Y.; Shin, H.; Kim, S.; Char, K.; Choi, J.W. Zn^{2+} -Imidazole Coordination Crosslinks for Elastic Polymeric Binders in High-Capacity Silicon Electrodes. *Adv. Sci.* **2021**, *8*, 2004290. [[CrossRef](#)]
173. Luo, P.; Lai, P.; Huang, Y.; Yuan, Y.; Wen, J.; Xie, C.; Li, J.; Liu, L. A Highly Stretchable and Self-Healing Composite Binder Based on the Hydrogen-Bond Network for Silicon Anodes in High-Energy-Density Lithium-Ion Batteries. *ChemElectroChem* **2022**, *9*, e202200155. [[CrossRef](#)]

174. Liu, M.; Chen, P.; Pan, X.; Pan, S.; Zhang, X.; Zhou, Y.; Bi, M.; Sun, J.; Yang, S.; Vasiliev, A.L.; et al. Synergism of Flame-Retardant, Self-Healing, High-Conductive and Polar to a Multi-Functional Binder for Lithium–Sulfur Batteries. *Adv. Funct. Mater.* **2022**, *32*, 2205031. [[CrossRef](#)]
175. Jiao, X.; Yin, J.; Xu, X.; Wang, J.; Liu, Y.; Xiong, S.; Zhang, Q.; Song, J. Highly Energy-Dissipative, Fast Self-Healing Binder for Stable Si Anode in Lithium-Ion Batteries. *Adv. Funct. Mater.* **2021**, *31*, 2005699. [[CrossRef](#)]
176. Liu, H.; Wu, Q.; Guan, X.; Liu, M.; Wang, F.; Li, R.; Xu, J. Ionically Conductive Self-Healing Polymer Binders with Poly(ether-thioureas) Segments for High-Performance Silicon Anodes in Lithium-Ion Batteries. *ACS Appl. Energy Mater.* **2022**, *5*, 4934–4944. [[CrossRef](#)]
177. Chen, H.; Wu, Z.; Su, Z.; Chen, S.; Yan, C.; Al-Mamun, M.; Tang, Y.; Zhang, S. A mechanically robust self-healing binder for silicon anode in lithium ion batteries. *Nano Energy* **2021**, *81*, 105654. [[CrossRef](#)]
178. Munaoka, T.; Yan, X.; Lopez, J.; To, J.W.F.; Park, J.; Tok, J.B.-H.; Cui, Y.; Bao, Z. Ionically Conductive Self-Healing Binder for Low Cost Si Microparticles Anodes in Li-Ion Batteries. *Adv. Energy Mater.* **2018**, *8*, 1703138. [[CrossRef](#)]
179. Wang, Y.; Xu, H.; Chen, X.; Jin, H.; Wang, J. Novel constructive self-healing binder for silicon anodes with high mass loading in lithium-ion batteries. *Energy Storage Mater.* **2021**, *38*, 121–129. [[CrossRef](#)]
180. Armand, M.; Tarascon, J.-M. Building better batteries. *Nature* **2008**, *451*, 652–657. [[CrossRef](#)]
181. Li, W.; Dahn, J.R.; Wainwright, D.S. Rechargeable Lithium Batteries with Aqueous Electrolytes. *Science* **1994**, *264*, 1115–1118. [[CrossRef](#)]
182. Zheng, F.; Kotobuki, M.; Song, S.; Lai, M.O.; Lu, L. Review on solid electrolytes for all-solid-state lithium-ion batteries. *J. Power Sources* **2018**, *389*, 198–213. [[CrossRef](#)]
183. Koerver, R.; Aygün, I.; Leichtweiß, T.; Dietrich, C.; Zhang, W.; Binder, J.O.; Hartmann, P.; Zeier, W.G.; Janek, J. Capacity Fade in Solid-State Batteries: Interphase Formation and Chemomechanical Processes in Nickel-Rich Layered Oxide Cathodes and Lithium Thiophosphate Solid Electrolytes. *Chem. Mater.* **2017**, *29*, 5574–5582. [[CrossRef](#)]
184. Kim, D.H.; Oh, D.Y.; Park, K.H.; Choi, Y.E.; Nam, Y.J.; Lee, H.A.; Lee, S.-M.; Jung, Y.S. Infiltration of Solution-Processable Solid Electrolytes into Conventional Li-Ion-Battery Electrodes for All-Solid-State Li-Ion Batteries. *Nano Lett.* **2017**, *17*, 3013–3020. [[CrossRef](#)]
185. Rosero-Navarro, N.C.; Kinoshita, T.; Miura, A.; Higuchi, M.; Tadanaga, K. Effect of the binder content on the electrochemical performance of composite cathode using $\text{Li}_6\text{PS}_5\text{Cl}$ precursor solution in an all-solid-state lithium battery. *Ionics (Kiel)* **2017**, *23*, 1619–1624. [[CrossRef](#)]
186. Lee, K.; Lee, J.; Choi, S.; Char, K.; Choi, J.W. Thiol–Ene Click Reaction for Fine Polarity Tuning of Polymeric Binders in Solution-Processed All-Solid-State Batteries. *ACS Energy Lett.* **2019**, *4*, 94–101. [[CrossRef](#)]
187. Lee, K.; Kim, S.; Park, J.; Park, S.H.; Coskun, A.; Jung, D.S.; Cho, W.; Choi, J.W. Selection of Binder and Solvent for Solution-Processed All-Solid-State Battery. *J. Electrochem. Soc.* **2017**, *164*, A2075–A2081. [[CrossRef](#)]
188. Zhang, J.; Zhong, H.; Zheng, C.; Xia, Y.; Liang, C.; Huang, H.; Gan, Y.; Tao, X.; Zhang, W. All-solid-state batteries with slurry coated $\text{LiNi}_{0.8}\text{Co}_{0.1}\text{Mn}_{0.1}\text{O}_2$ composite cathode and $\text{Li}_6\text{PS}_5\text{Cl}$ electrolyte: Effect of binder content. *J. Power Sources* **2018**, *391*, 73–79. [[CrossRef](#)]
189. Wan, Z.; Lei, D.; Yang, W.; Liu, C.; Shi, K.; Hao, X.; Shen, L.; Lv, W.; Li, B.; Yang, Q.H.; et al. Low Resistance–Integrated All-Solid-State Battery Achieved by $\text{Li}_7\text{La}_3\text{Zr}_2\text{O}_{12}$ Nanowire Upgrading Polyethylene Oxide (PEO) Composite Electrolyte and PEO Cathode Binder. *Adv. Funct. Mater.* **2019**, *29*, 1805301. [[CrossRef](#)]
190. Park, K.H.; Bai, Q.; Kim, D.H.; Oh, D.Y.; Zhu, Y.; Mo, Y.; Jung, Y.S. Design Strategies, Practical Considerations, and New Solution Processes of Sulfide Solid Electrolytes for All-Solid-State Batteries. *Adv. Energy Mater.* **2018**, *8*, 1800035. [[CrossRef](#)]
191. Chen, R.-J.; Zhang, Y.-B.; Liu, T.; Xu, B.-Q.; Lin, Y.-H.; Nan, C.-W.; Shen, Y. Addressing the Interface Issues in All-Solid-State Bulk-Type Lithium Ion Battery via an All-Composite Approach. *ACS Appl. Mater. Interfaces* **2017**, *9*, 9654–9661. [[CrossRef](#)]
192. Wang, K.; Ye, Q.; Zhang, J.; Huang, H.; Gan, Y.; He, X.; Zhang, W. Halide Electrolyte Li_3InCl_6 -Based All-Solid-State Lithium Batteries with Slurry-Coated $\text{LiNi}_{0.8}\text{Co}_{0.1}\text{Mn}_{0.1}\text{O}_2$ Composite Cathode: Effect of Binders. *Front. Mater.* **2021**, *8*, 727617. [[CrossRef](#)]
193. Ai, G.; Dai, Y.; Ye, Y.; Mao, W.; Wang, Z.; Zhao, H.; Chen, Y.; Zhu, J.; Fu, Y.; Battaglia, V.; et al. Investigation of surface effects through the application of the functional binders in lithium sulfur batteries. *Nano Energy* **2015**, *16*, 28–37. [[CrossRef](#)]
194. Ling, M.; Xu, Y.; Zhao, H.; Gu, X.; Qiu, J.; Li, S.; Wu, M.; Song, X.; Yan, C.; Liu, G.; et al. Dual-functional gum arabic binder for silicon anodes in lithium ion batteries. *Nano Energy* **2015**, *12*, 178–185. [[CrossRef](#)]
195. Koo, B.; Kim, H.; Cho, Y.; Lee, K.T.; Choi, N.; Cho, J. A Highly Cross-Linked Polymeric Binder for High-Performance Silicon Negative Electrodes in Lithium Ion Batteries. *Angew. Chem. Int. Ed.* **2012**, *51*, 8762–8767. [[CrossRef](#)]
196. Ito, S.; Fujiki, S.; Yamada, T.; Aihara, Y.; Park, Y.; Kim, T.Y.; Baek, S.-W.; Lee, J.-M.; Doo, S.; Machida, N. A rocking chair type all-solid-state lithium ion battery adopting $\text{Li}_2\text{O}-\text{ZrO}_2$ coated $\text{LiNi}_{0.8}\text{Co}_{0.15}\text{Al}_{0.05}\text{O}_2$ and a sulfide based electrolyte. *J. Power Sources* **2014**, *248*, 943–950. [[CrossRef](#)]
197. Inada, T. Fabrications and properties of composite solid-state electrolytes. *Solid State Ion.* **2003**, *158*, 275–280. [[CrossRef](#)]
198. Banerjee, A.; Park, K.H.; Heo, J.W.; Nam, Y.J.; Moon, C.K.; Oh, S.M.; Hong, S.-T.; Jung, Y.S. Na_3SbS_4 : A Solution Processable Sodium Superionic Conductor for All-Solid-State Sodium-Ion Batteries. *Angew. Chem. Int. Ed.* **2016**, *55*, 9634–9638. [[CrossRef](#)] [[PubMed](#)]
199. Park, K.H.; Oh, D.Y.; Choi, Y.E.; Nam, Y.J.; Han, L.; Kim, J.-Y.; Xin, H.; Lin, F.; Oh, S.M.; Jung, Y.S. Solution-Processable Glass $\text{LiI-Li}_4\text{SnS}_4$ Superionic Conductors for All-Solid-State Li-Ion Batteries. *Adv. Mater.* **2016**, *28*, 1874–1883. [[CrossRef](#)] [[PubMed](#)]

200. Nam, Y.J.; Oh, D.Y.; Jung, S.H.; Jung, Y.S. Toward practical all-solid-state lithium-ion batteries with high energy density and safety: Comparative study for electrodes fabricated by dry- and slurry-mixing processes. *J. Power Sources* **2018**, *375*, 93–101. [CrossRef]
201. Li, C.; Zhang, H.; Otaegui, L.; Singh, G.; Armand, M.; Rodriguez-Martinez, L.M. Estimation of energy density of Li-S batteries with liquid and solid electrolytes. *J. Power Sources* **2016**, *326*, 1–5. [CrossRef]
202. Hippauf, F.; Schumm, B.; Doerfler, S.; Althues, H.; Fujiki, S.; Shiratsuchi, T.; Tsujimura, T.; Aihara, Y.; Kaskel, S. Overcoming binder limitations of sheet-type solid-state cathodes using a solvent-free dry-film approach. *Energy Storage Mater.* **2019**, *21*, 390–398. [CrossRef]
203. Zhang, Z.; Wu, L.; Zhou, D.; Weng, W.; Yao, X. Flexible Sulfide Electrolyte Thin Membrane with Ultrahigh Ionic Conductivity for All-Solid-State Lithium Batteries. *Nano Lett.* **2021**, *21*, 5233–5239. [CrossRef] [PubMed]
204. Li, Y.; Wu, Y.; Ma, T.; Wang, Z.; Gao, Q.; Xu, J.; Chen, L.; Li, H.; Wu, F. Long-Life Sulfide All-Solid-State Battery Enabled by Substrate-Modulated Dry-Process Binder. *Adv. Energy Mater.* **2022**, *12*, 2201732. [CrossRef]
205. Wang, H.; Wu, L.; Xue, B.; Wang, F.; Luo, Z.; Zhang, X.; Calvez, L.; Fan, P.; Fan, B. Improving Cycling Stability of the Lithium Anode by a Spin-Coated High-Purity Li₃PS₄ Artificial SEI Layer. *ACS Appl. Mater. Interfaces* **2022**, *14*, 15214–15224. [CrossRef] [PubMed]
206. Liu, S.; Zhou, L.; Han, J.; Wen, K.; Guan, S.; Xue, C.; Zhang, Z.; Xu, B.; Lin, Y.; Shen, Y.; et al. Super Long-Cycling All-Solid-State Battery with Thin Li₆PS₅Cl-Based Electrolyte. *Adv. Energy Mater.* **2022**, *12*, 2200660. [CrossRef]
207. Inada, T.; Kobayashi, T.; Sonoyama, N.; Yamada, A.; Kondo, S.; Nagao, M.; Kanno, R. All solid-state sheet battery using lithium inorganic solid electrolyte, thio-LISICON. *J. Power Sources* **2009**, *194*, 1085–1088. [CrossRef]
208. Wang, C.; Kim, J.T.; Wang, C.; Sun, X. Progress and Prospects of Inorganic Solid-State Electrolyte-Based All-Solid-State Pouch Cells. *Adv. Mater.* **2023**, *35*, 2209074. [CrossRef] [PubMed]
209. Fan, B.; Fang, Y.; Xue, B.; Wu, Q.; Luo, Z.; Zhang, X.; Calvez, L.; Wu, L. Spray-Printed Flexible Li₂S Cathode with Inorganic Ion-Conductive Binder Nano-Li₃PS₄. *ACS Appl. Mater. Interfaces* **2024**, *16*, 7182–7188. [CrossRef]
210. Liang, J.; Chen, D.; Adair, K.; Sun, Q.; Holmes, N.G.; Zhao, Y.; Sun, Y.; Luo, J.; Li, R.; Zhang, L.; et al. Insight into Prolonged Cycling Life of 4 V All-Solid-State Polymer Batteries by a High-Voltage Stable Binder. *Adv. Energy Mater.* **2021**, *11*, 2002455. [CrossRef]
211. Yang, X.; Sun, Q.; Zhao, C.; Gao, X.; Adair, K.R.; Liu, Y.; Luo, J.; Lin, X.; Liang, J.; Huang, H.; et al. High-areal-capacity all-solid-state lithium batteries enabled by rational design of fast ion transport channels in vertically-aligned composite polymer electrodes. *Nano Energy* **2019**, *61*, 567–575. [CrossRef]
212. Ma, J.; Liu, Z.; Chen, B.; Wang, L.; Yue, L.; Liu, H.; Zhang, J.; Liu, Z.; Cui, G. A Strategy to Make High Voltage LiCoO₂ Compatible with Polyethylene Oxide Electrolyte in All-Solid-State Lithium Ion Batteries. *J. Electrochem. Soc.* **2017**, *164*, A3454–A3461. [CrossRef]
213. Miyashiro, H.; Kobayashi, Y.; Seki, S.; Mita, Y.; Usami, A.; Nakayama, M.; Wakihara, M. Fabrication of All-Solid-State Lithium Polymer Secondary Batteries Using Al₂O₃-Coated LiCoO₂. *Chem. Mater.* **2005**, *17*, 5603–5605. [CrossRef]
214. Hovington, P.; Lagacé, M.; Guerfi, A.; Bouchard, P.; Mauger, A.; Julien, C.M.; Armand, M.; Zaghib, K. New Lithium Metal Polymer Solid State Battery for an Ultrahigh Energy: Nano C-LiFePO₄ versus Nano Li_{1.2}V₃O₈. *Nano Lett.* **2015**, *15*, 2671–2678. [CrossRef] [PubMed]
215. Murugan, R.; Thangadurai, V.; Weppner, W. Fast Lithium Ion Conduction in Garnet-Type Li₇La₃Zr₂O₁₂. *Angew. Chem. Int. Ed.* **2007**, *46*, 7778–7781. [CrossRef] [PubMed]
216. Thangadurai, V.; Narayanan, S.; Pinzaru, D. Garnet-type solid-state fast Li ion conductors for Li batteries: Critical review. *Chem. Soc. Rev.* **2014**, *43*, 4714. [CrossRef] [PubMed]
217. Jia, M.; Guo, Y.; Bian, H.; Zhang, Q.; Zhang, L.; Zhang, S. An ultra-stable lithium plating process enabled by the nanoscale interphase of a macromolecular additive. *J. Mater. Chem. A Mater.* **2020**, *8*, 23844–23850. [CrossRef]
218. Wang, R.; Feng, L.; Yang, W.; Zhang, Y.; Zhang, Y.; Bai, W.; Liu, B.; Zhang, W.; Chuan, Y.; Zheng, Z.; et al. Effect of Different Binders on the Electrochemical Performance of Metal Oxide Anode for Lithium-Ion Batteries. *Nanoscale Res. Lett.* **2017**, *12*, 575. [CrossRef] [PubMed]
219. Wu, F.; Li, W.; Chen, L.; Lu, Y.; Su, Y.; Bao, W.; Wang, J.; Chen, S.; Bao, L. Polyacrylonitrile-polyvinylidene fluoride as high-performance composite binder for layered Li-rich oxides. *J. Power Sources* **2017**, *359*, 226–233. [CrossRef]
220. Manickam, M.; Takata, M. Effect of cathode binder on capacity retention and cycle life in transition metal phosphate of a rechargeable lithium battery. *Electrochim. Acta* **2003**, *48*, 957–963. [CrossRef]
221. Zhang, Y.; Huld, F.; Lu, S.; Jektvik, C.; Lou, F.; Yu, Z. Revisiting Polytetrafluoroethylene Binder for Solvent-Free Lithium-Ion Battery Anode Fabrication. *Batteries* **2022**, *8*, 57. [CrossRef]
222. Yim, T.; Choi, S.J.; Jo, Y.N.; Kim, T.H.; Kim, K.J.; Jeong, G.; Kim, Y.J. Effect of binder properties on electrochemical performance for silicon-graphite anode: Method and application of binder screening. *Electrochim. Acta* **2014**, *136*, 112–120. [CrossRef]
223. Wei, L.; Chen, C.; Hou, Z.; Wei, H. Poly(acrylic acid sodium) grafted carboxymethyl cellulose as a high performance polymer binder for silicon anode in lithium ion batteries. *Sci. Rep.* **2016**, *6*, 19583. [CrossRef]
224. Rajeev, K.K.; Kim, E.; Nam, J.; Lee, S.; Mun, J.; Kim, T.-H. Chitosan-grafted-polyaniline copolymer as an electrically conductive and mechanically stable binder for high-performance Si anodes in Li-ion batteries. *Electrochim. Acta* **2020**, *333*, 135532. [CrossRef]
225. Nagulapati, V.M.; Lee, J.H.; Kim, H.S.; Oh, J.; Kim, I.T.; Hur, J.; Lee, S.G. Novel hybrid binder mixture tailored to enhance the electrochemical performance of SbTe bi-metallic anode for sodium ion batteries. *J. Electroanal. Chem.* **2020**, *865*, 114160. [CrossRef]

226. Xiao, W.; Sun, Q.; Banis, M.N.; Wang, B.; Li, W.; Li, M.; Lushington, A.; Li, R.; Li, X.; Sham, T.K.; et al. Understanding the Critical Role of Binders in Phosphorus/Carbon Anode for Sodium-Ion Batteries through Unexpected Mechanism. *Adv. Funct. Mater.* **2020**, *30*, 2000060. [[CrossRef](#)]
227. Mao, Z.; Wang, R.; He, B.; Jin, J.; Gong, Y.; Wang, H. Cross-Linked Sodium Alginate as A Multifunctional Binder to Achieve High-Rate and Long-Cycle Stability for Sodium-Ion Batteries. *Small* **2023**, *19*, 2207224. [[CrossRef](#)]
228. Feng, J.; Wang, L.; Li, D.; Lu, P.; Hou, F.; Liang, J. Enhanced electrochemical stability of carbon-coated antimony nanoparticles with sodium alginate binder for sodium-ion batteries. *Prog. Nat. Sci. Mater. Int.* **2018**, *28*, 205–211. [[CrossRef](#)]
229. Yao, Q.; Zhu, Y.; Zheng, C.; Wang, N.; Wang, D.; Tian, F.; Bai, Z.; Yang, J.; Qian, Y.; Dou, S. Intermolecular Cross-Linking Reinforces Polymer Binders for Durable Alloy-Type Anode Materials of Sodium-Ion Batteries. *Adv. Energy Mater.* **2023**, *13*, 2202939. [[CrossRef](#)]
230. Ni, D.; Sun, W.; Lu, C.; Wang, Z.; Qiao, J.; Cai, H.; Liu, C.; Sun, K. Improved rate and cycling performance of FeF₂-rGO hybrid cathode with poly (acrylic acid) binder for sodium ion batteries. *J. Power Sources* **2019**, *413*, 449–458. [[CrossRef](#)]
231. Dai, K.; Zhao, H.; Wang, Z.; Song, X.; Battaglia, V.; Liu, G. Toward high specific capacity and high cycling stability of pure tin nanoparticles with conductive polymer binder for sodium ion batteries. *J. Power Sources* **2014**, *263*, 276–279. [[CrossRef](#)]
232. Kim, K.T.; Kwon, T.Y.; Song, Y.B.; Kim, S.M.; Byun, S.C.; Min, H.S.; Kim, S.H.; Jung, Y.S. Wet-slurry fabrication using PVdF-HFP binder with sulfide electrolytes via synergetic cosolvent approach for all-solid-state batteries. *Chem. Eng. J.* **2022**, *450*, 138047. [[CrossRef](#)]
233. Zhao, X.; Shen, L.; Zhang, N.; Yang, J.; Liu, G.; Wu, J.; Yao, X. Stable Binder Boosting Sulfide Solid Electrolyte Thin Membrane for All-Solid-State Lithium Batteries. *Energy Mater. Adv.* **2024**, *5*, 0074. [[CrossRef](#)]
234. Yang, Y.; Wu, S.; Zhang, Y.; Liu, C.; Wei, X.; Luo, D.; Lin, Z. Towards efficient binders for silicon based lithium-ion battery anodes. *Chem. Eng. J.* **2021**, *406*, 126807. [[CrossRef](#)]
235. Jin, H.-J.; Lee, J.; Yoon, J.; Kim, H.; Kim, J. Polymeric Binder Design for Sustainable Lithium-ion Battery Chemistry. *Polymers* **2024**, *16*, 254. [[CrossRef](#)] [[PubMed](#)]
236. Vogl, U.S.; Das, P.K.; Weber, A.Z.; Winter, M.; Kostecki, R.; Lux, S.F. Mechanism of Interactions between CMC Binder and Si Single Crystal Facets. *Langmuir* **2014**, *30*, 10299–10307. [[CrossRef](#)] [[PubMed](#)]
237. Mark, J.E. (Ed.) *Physical Properties of Polymers Handbook*; Springer: New York, NY, USA, 2007. [[CrossRef](#)]
238. Chen, L.; Xie, X.; Xie, J.; Wang, K.; Yang, J. Binder effect on cycling performance of silicon/carbon composite anodes for lithium ion batteries. *J. Appl. Electrochem.* **2006**, *36*, 1099–1104. [[CrossRef](#)]
239. Yao, D.; Feng, J.; Wang, J.; Deng, Y.; Wang, C. Synthesis of silicon anode binders with ultra-high content of catechol groups and the effect of molecular weight on battery performance. *J. Power Sources* **2020**, *463*, 228188. [[CrossRef](#)]
240. Liu, Y.; He, D.; Tan, Q.; Wan, Q.; Han, K.; Liu, Z.; Li, P.; An, F.; Qu, X. A synergistic strategy for an advanced electrode with Fe₃O₄ embedded in a 3D N-doped porous graphene framework and a strong adhesive binder for lithium/potassium ion batteries with an ultralong cycle lifespan. *J. Mater. Chem. A Mater.* **2019**, *7*, 19430–19441. [[CrossRef](#)]
241. Li, M.; Zhang, J.; Gao, Y.; Wang, X.; Zhang, Y.; Zhang, S. A water-soluble, adhesive and 3D cross-linked polyelectrolyte binder for high-performance lithium–sulfur batteries. *J. Mater. Chem. A Mater.* **2021**, *9*, 2375–2384. [[CrossRef](#)]
242. Hitomi, S.; Kubota, K.; Horiba, T.; Hida, K.; Matsuyama, T.; Oji, H.; Yasuno, S.; Komaba, S. Application of Acrylic-Rubber-Based Latex Binder to High-Voltage Spinel Electrodes of Lithium-Ion Batteries. *ChemElectroChem* **2019**, *6*, 5070–5079. [[CrossRef](#)]
243. Choi, J.; Kim, K.; Jeong, J.; Cho, K.Y.; Ryoo, M.-H.; Lee, Y.M. Highly Adhesive and Soluble Copolyimide Binder: Improving the Long-Term Cycle Life of Silicon Anodes in Lithium-Ion Batteries. *ACS Appl. Mater. Interfaces* **2015**, *7*, 14851–14858. [[CrossRef](#)]
244. Zhang, T.; Li, J.; Liu, J.; Deng, Y.; Wu, Z.; Yin, Z.; Guo, D.; Huang, L.; Sun, S. Suppressing the voltage-fading of layered lithium-rich cathode materials via an aqueous binder for Li-ion batteries. *Chem. Commun.* **2016**, *52*, 4683–4686. [[CrossRef](#)] [[PubMed](#)]
245. Liu, T.; Chu, Q.; Yan, C.; Zhang, S.; Lin, Z.; Lu, J. Interweaving 3D Network Binder for High-Areal-Capacity Si Anode through Combined Hard and Soft Polymers. *Adv. Energy Mater.* **2019**, *9*, 1802645. [[CrossRef](#)]
246. Jeong, Y.K.; Choi, J.W. Mussel-Inspired Self-Healing Metallocopolymers for Silicon Nanoparticle Anodes. *ACS Nano* **2019**, *13*, 8364–8373. [[CrossRef](#)] [[PubMed](#)]
247. Yuca, N.; Cetintasoglu, M.E.; Dogdu, M.F.; Akbulut, H.; Tabanli, S.; Colak, U.; Taskin, O.S. Highly efficient poly(fluorene phenylene) copolymer as a new class of binder for high-capacity silicon anode in lithium-ion batteries. *Int. J. Energy Res.* **2018**, *42*, 1148–1157. [[CrossRef](#)]
248. Zhang, Q.; Chen, J.; Jin, B.; Peng, R. A new linear heptafluoro glycidyl ether binder: Synthesis, characterization, and mechanical properties. *Macromol. Res.* **2023**, *31*, 699–709. [[CrossRef](#)]
249. Liu, J.; Galpaya, D.G.D.; Yan, L.; Sun, M.; Lin, Z.; Yan, C.; Liang, C.; Zhang, S. Exploiting a robust biopolymer network binder for an ultrahigh-areal-capacity Li–S battery. *Energy Environ. Sci.* **2017**, *10*, 750–755. [[CrossRef](#)]
250. Shin, D.; Park, H.; Paik, U. Cross-linked poly(acrylic acid)-carboxymethyl cellulose and styrene-butadiene rubber as an efficient binder system and its physicochemical effects on a high energy density graphite anode for Li-ion batteries. *Electrochim. Commun.* **2017**, *77*, 103–106. [[CrossRef](#)]
251. Zou, F.; Manthiram, A. A Review of the Design of Advanced Binders for High-Performance Batteries. *Adv. Energy Mater.* **2020**, *10*, 2002508. [[CrossRef](#)]
252. Ahn, J.; Im, H.G.; Lee, Y.; Lee, D.; Jang, H.; Oh, Y.; Chung, K.; Park, T.; Um, M.K.; Yi, J.W.; et al. A novel organosilicon-type binder for LiCoO₂ cathode in Li-ion batteries. *Energy Storage Mater.* **2022**, *49*, 58–66. [[CrossRef](#)]

253. Shi, Y.; Gao, F.; Xie, Y.; Xu, X.; Li, F.; Han, X.; Yao, X.; Wang, D.; Hou, Y.; Gao, X.; et al. In situ interlocked gradient adaptive network binder with robust adhesion and cycle performance for silicon anodes. *J. Power Sources* **2023**, *580*, 233267. [CrossRef]
254. Wang, Y.; Dang, D.; Li, D.; Hu, J.; Cheng, Y.-T. Influence of polymeric binders on mechanical properties and microstructure evolution of silicon composite electrodes during electrochemical cycling. *J. Power Sources* **2019**, *425*, 170–178. [CrossRef]
255. Cholewinski, A.; Si, P.; Uceda, M.; Pope, M.; Zhao, B. Polymer Binders: Characterization and Development toward Aqueous Electrode Fabrication for Sustainability. *Polymers* **2021**, *13*, 631. [CrossRef] [PubMed]
256. Sun, C.; Liu, J.; Gong, Y.; Wilkinson, D.P.; Zhang, J. Recent advances in all-solid-state rechargeable lithium batteries. *Nano Energy* **2017**, *33*, 363–386. [CrossRef]
257. Liew, C.; Durairaj, R.; Ramesh, S. Rheological Studies of PMMA–PVC Based Polymer Blend Electrolytes with LiTFSI as Doping Salt. *PLoS ONE* **2014**, *9*, e102815. [CrossRef] [PubMed]
258. Han, L.; Lehmann, M.L.; Zhu, J.; Liu, T.; Zhou, Z.; Tang, X.; Heish, C.T.; Sokolov, A.P.; Cao, P.; Chen, X.C.; et al. Recent Developments and Challenges in Hybrid Solid Electrolytes for Lithium-Ion Batteries. *Front. Energy Res.* **2020**, *8*, 202. [CrossRef]
259. He, R.; Kyu, T. Effect of Plasticization on Ionic Conductivity Enhancement in Relation to Glass Transition Temperature of Crosslinked Polymer Electrolyte Membranes. *Macromolecules* **2016**, *49*, 5637–5648. [CrossRef]
260. Shetty, S.K.; Ismayil; Noor, I.M. Effect of new crystalline phase on the ionic conduction properties of sodium perchlorate salt doped carboxymethyl cellulose biopolymer electrolyte films. *J. Polym. Res.* **2021**, *28*, 415. [CrossRef]
261. Olmedo-Martínez, J.; Meabe, L.; Basterretxea, A.; Mecerreyres, D.; Müller, A. Effect of Chemical Structure and Salt Concentration on the Crystallization and Ionic Conductivity of Aliphatic Polyethers. *Polymers* **2019**, *11*, 452. [CrossRef]
262. Yim, T.; Choi, S.J.; Park, J.H.; Cho, W.; Jo, Y.N.; Kim, T.H.; Kim, Y.J. The effect of an elastic functional group in a rigid binder framework of silicon–graphite composites on their electrochemical performance. *Phys. Chem. Chem. Phys.* **2015**, *17*, 2388–2393. [CrossRef]
263. Jenkins, C.A.; Coles, S.R.; Loveridge, M.J. Investigation into Durable Polymers with Enhanced Toughness and Elasticity for Application in Flexible Li-Ion Batteries. *ACS Appl. Energy Mater.* **2020**, *3*, 12494–12505. [CrossRef]
264. Zeng, W.; Wang, L.; Peng, X.; Liu, T.; Jiang, Y.; Qin, F.; Hu, L.; Chu, P.K.; Huo, K.; Zhou, Y. Enhanced Ion Conductivity in Conducting Polymer Binder for High-Performance Silicon Anodes in Advanced Lithium-Ion Batteries. *Adv. Energy Mater.* **2018**, *8*, 1702314. [CrossRef]
265. Qiu, D.; Guan, J.; Li, M.; Kang, C.; Wei, J.; Li, Y.; Xie, Z.; Wang, F.; Yang, R. Kinetics Enhanced Nitrogen-Doped Hierarchical Porous Hollow Carbon Spheres Boosting Advanced Potassium-Ion Hybrid Capacitors. *Adv. Funct. Mater.* **2019**, *29*, 1903496. [CrossRef]
266. Kovalenko, I.; Zdryko, B.; Magasinski, A.; Hertzberg, B.; Milicev, Z.; Burtovyy, R.; Luzinov, I.; Yushin, G. A Major Constituent of Brown Algae for Use in High-Capacity Li-Ion Batteries. *Science* **2011**, *334*, 75–79. [CrossRef] [PubMed]
267. Vorobeva, K.A.; Eliseeva, S.N.; Apraksin, R.V.; Kamenskii, M.A.; Tolstopiatova, E.G.; Kondratiev, V.V. Improved electrochemical properties of cathode material LiMn₂O₄ with conducting polymer binder. *J. Alloys Compd.* **2018**, *766*, 33–44. [CrossRef]
268. Eom, J.-Y.; Cao, L. Effect of anode binders on low-temperature performance of automotive lithium-ion batteries. *J. Power Sources* **2019**, *441*, 227178. [CrossRef]
269. Younesi, R.; Hahlin, M.; Treskow, M.; Scheers, J.; Johansson, P.; Edström, K. Ether Based Electrolyte, LiB(CN)₄ Salt and Binder Degradation in the Li–O₂ Battery Studied by Hard X-ray Photoelectron Spectroscopy (HAXPES). *J. Phys. Chem. C* **2012**, *116*, 18597–18604. [CrossRef]
270. Le, A.V.; Wang, M.; Noelle, D.J.; Shi, Y.; Meng, Y.S.; Wu, D.; Fan, J.; Qiao, Y. Using high-HFP-content cathode binder for mitigation of heat generation of lithium-ion battery. *Int. J. Energy Res.* **2017**, *41*, 2430–2438. [CrossRef]
271. Komoda, Y.; Ishibashi, K.; Kuratani, K.; Suzuki, K.; Ohmura, N.; Kobayashi, H. Effects of drying rate and slurry microstructure on the formation process of LiB cathode and electrochemical properties. *J. Power Sources* **2023**, *568*, 232983. [CrossRef]
272. Lu, L.; Han, X.; Li, J.; Hua, J.; Ouyang, M. A review on the key issues for lithium-ion battery management in electric vehicles. *J. Power Sources* **2013**, *226*, 272–288. [CrossRef]
273. Su, C.; Gao, X. Recent Advances in Battery Binders with an Insight of Predictive Commercial Development. In *Electronics, Communications and Networks: Proceedings of the 13th International Conference (CECNet 2023), Macao, China, 17–20 November 2023*; IOS Press: Amsterdam, The Netherlands, 2024. [CrossRef]
274. Lim, S.; Chu, H.; Lee, K.; Yim, T.; Kim, Y.J.; Mun, J.; Kim, T.H. Physically Cross-linked Polymer Binder Induced by Reversible Acid–Base Interaction for High-Performance Silicon Composite Anodes. *ACS Appl. Mater. Interfaces* **2015**, *7*, 23545–23553. [CrossRef]
275. Kim, H.-M.; Yoo, B.-I.; Yi, J.-W.; Choi, M.-J.; Yoo, J.-K. Solvent-Free Fabrication of Thick Electrodes in Thermoplastic Binders for High Energy Density Lithium-Ion Batteries. *Nanomaterials* **2022**, *12*, 3320. [CrossRef] [PubMed]
276. Ruschaupt, P.; Pohlmann, S.; Varzi, A.; Passerini, S. Determining Realistic Electrochemical Stability Windows of Electrolytes for Electrical Double-Layer Capacitors. *Batter. Supercaps* **2020**, *3*, 698–707. [CrossRef]
277. Liang, X.; Ahmad, N.; Zhang, B.; Zeng, C.; Cao, X.; Dong, Q.; Yang, W. Research progress of robust binders with superior mechanical properties for high-performance silicon-based lithium-ion batteries. *Mater. Chem. Front.* **2024**, *8*, 1480–1512. [CrossRef]
278. Yan, X.; Zhang, Y.; Zhu, K.; Gao, Y.; Zhang, D.; Chen, G.; Wang, C.; Wei, Y. Enhanced electrochemical properties of TiO₂(B) nanoribbons using the styrene butadiene rubber and sodium carboxyl methyl cellulose water binder. *J. Power Sources* **2014**, *246*, 95–102. [CrossRef]

279. Hong, X.; Jin, J.; Wen, Z.; Zhang, S.; Wang, Q.; Shen, C.; Rui, K. On the dispersion of lithium-sulfur battery cathode materials effected by electrostatic and stereo-chemical factors of binders. *J. Power Sources* **2016**, *324*, 455–461. [[CrossRef](#)]
280. Nakazawa, T.; Ikoma, A.; Kido, R.; Ueno, K.; Dokko, K.; Watanabe, M. Effects of compatibility of polymer binders with solvate ionic liquid electrolytes on discharge and charge reactions of lithium-sulfur batteries. *J. Power Sources* **2016**, *307*, 746–752. [[CrossRef](#)]
281. Yang, Z.; Guo, M.; Meng, P.; Jiang, M.; Qiu, X.; Zhang, J.; Fu, C. Aqueous Binders Compatible with Ionic Liquid Electrolyte for High-Performance Aluminum-Ion Batteries. *Chem. Eur. J.* **2023**, *29*, e202203546. [[CrossRef](#)]
282. Xing, J.; Bliznakov, S.; Bonville, L.; Oljaca, M.; Maric, R. A Review of Nonaqueous Electrolytes, Binders, and Separators for Lithium-Ion Batteries. *Electrochem. Energy Rev.* **2022**, *5*, 14. [[CrossRef](#)]
283. Tron, A.; Hamid, R.; Zhang, N.; Paolella, A.; Wulfert-Holzmann, P.; Kolotygin, V.; López-Aranguren, P.; Beutl, A. Film processing of Li₆PS₅Cl electrolyte using different binders and their combinations. *J. Energy Storage* **2023**, *66*, 107480. [[CrossRef](#)]
284. Drago, R.S.; Vogel, G.C.; Needham, T.E. Four-parameter equation for predicting enthalpies of adduct formation. *J. Am. Chem. Soc.* **1971**, *93*, 6014–6026. [[CrossRef](#)]
285. Pizzi, A.; Mtsweni, B.; Parsons, W. Wood-induced catalytic activation of PF adhesives autopolymerization vs. PF/wood covalent bonding. *J. Appl. Polym. Sci.* **1994**, *52*, 1847–1856. [[CrossRef](#)]
286. Derjaguin, B.V.; Aleinikova, I.N.; Toporov, Y.P. On the role of electrostatic forces in the adhesion of polymer particles to solid surfaces. *Powder Technol.* **1969**, *2*, 154–158. [[CrossRef](#)]
287. McBain, J.W.; Hopkins, D.G. On Adhesives and Adhesive Action. *J. Phys. Chem.* **1925**, *29*, 188–204. [[CrossRef](#)]
288. Gardner, D.J.; Blumentritt, M.; Wang, L.; Yildirim, N. Adhesion Theories in Wood Adhesive Bonding. In *Progress in Adhesion and Adhesives*; Wiley: Hoboken, NJ, USA, 2015; pp. 125–168. [[CrossRef](#)]
289. Shi, Q.; Wong, S.-C.; Ye, W.; Hou, J.; Zhao, J.; Yin, J. Mechanism of Adhesion between Polymer Fibers at Nanoscale Contacts. *Langmuir* **2012**, *28*, 4663–4671. [[CrossRef](#)]
290. Léger, L.; Creton, C. Adhesion mechanisms at soft polymer interfaces. *Philos. Trans. R. Soc. A Math. Phys. Eng. Sci.* **2008**, *366*, 1425–1442. [[CrossRef](#)] [[PubMed](#)]
291. Fourche, G. An overview of the basic aspects of polymer adhesion. Part I: Fundamentals. *Polym. Eng. Sci.* **1995**, *35*, 957–967. [[CrossRef](#)]
292. Licari, J.J.; Swanson, D.W. Functions and theory of adhesives. In *Adhesives Technology for Electronic Applications*; Elsevier: Amsterdam, The Netherlands, 2011; pp. 35–74. [[CrossRef](#)]
293. Qin, T.; Yang, H.; Li, Q.; Yu, X.; Li, H. Design of functional binders for high-specific-energy lithium-ion batteries: From molecular structure to electrode properties. *Ind. Chem. Mater.* **2024**, *2*, 191–225. [[CrossRef](#)]
294. Xiao, X.; Wu, W.; Huang, X. A multi-scale approach for the stress analysis of polymeric separators in a lithium-ion battery. *J. Power Sources* **2010**, *195*, 7649–7660. [[CrossRef](#)]
295. Vetter, J.; Novák, P.; Wagner, M.R.; Veit, C.; Möller, K.-C.; Besenhard, J.O.; Winter, M.; Wohlfahrt-Mehrens, M.; Vogler, C.; Hammouche, A. Ageing mechanisms in lithium-ion batteries. *J. Power Sources* **2005**, *147*, 269–281. [[CrossRef](#)]
296. Park, H.-K.; Kong, B.-S.; Oh, E.-S. Effect of high adhesive polyvinyl alcohol binder on the anodes of lithium ion batteries. *Electrochim. Commun.* **2011**, *13*, 1051–1053. [[CrossRef](#)]
297. Guerfi, A.; Kaneko, M.; Petitclerc, M.; Mori, M.; Zaghib, K. LiFePO₄ water-soluble binder electrode for Li-ion batteries. *J. Power Sources* **2007**, *163*, 1047–1052. [[CrossRef](#)]
298. Chou, S.-L.; Pan, Y.; Wang, J.-Z.; Liu, H.-K.; Dou, S.-X. Small things make a big difference: Binder effects on the performance of Li and Na batteries. *Phys. Chem. Chem. Phys.* **2014**, *16*, 20347–20359. [[CrossRef](#)] [[PubMed](#)]
299. Foster, J.M.; Huang, X.; Jiang, M.; Chapman, S.J.; Protas, B.; Richardson, G. Causes of binder damage in porous battery electrodes and strategies to prevent it. *J. Power Sources* **2017**, *350*, 140–151. [[CrossRef](#)]
300. Han, D.; Han, I.K.; Son, H.B.; Kim, Y.S.; Ryu, J.; Park, S. Layering Charged Polymers Enable Highly Integrated High-Capacity Battery Anodes (Adv. Funct. Mater. 17/2023). *Adv. Funct. Mater.* **2023**, *33*, 2213458. [[CrossRef](#)]
301. Li, H.; Peng, L.; Wu, D.; Wu, J.; Zhu, Y.; Hu, X. Ultrahigh-Capacity and Fire-Resistant LiFePO₄-Based Composite Cathodes for Advanced Lithium-Ion Batteries. *Adv. Energy Mater.* **2019**, *9*, 1802930. [[CrossRef](#)]
302. Hu, L.; Jin, M.; Zhang, Z.; Chen, H.; Ajdari, F.B.; Song, J. Interface-Adaptive Binder Enabled by Supramolecular Interactions for High-Capacity Si/C Composite Anodes in Lithium-Ion Batteries. *Adv. Funct. Mater.* **2022**, *32*, 2111560. [[CrossRef](#)]
303. Cho, Y.; Kim, J.; Elabd, A.; Choi, S.; Park, K.; Kwon, T.-W.; Lee, J.; Char, K.; Coskun, A.; Choi, J.W. A Pyrene–Poly(acrylic acid)–Polyrotaxane Supramolecular Binder Network for High-Performance Silicon Negative Electrodes. *Adv. Mater.* **2019**, *31*, 1905048. [[CrossRef](#)] [[PubMed](#)]
304. Jin, J.; Shi, Z.; Wang, C. Electrochemical Performance of Electrospun carbon nanofibers as free-standing and binder-free anodes for Sodium-Ion and Lithium-Ion Batteries. *Electrochim. Acta* **2014**, *141*, 302–310. [[CrossRef](#)]
305. Kang, Y.; Deng, C.; Chen, Y.; Liu, X.; Liang, Z.; Li, T.; Hu, Q.; Zhao, Y. Binder-Free Electrodes and Their Application for Li-Ion Batteries. *Nanoscale Res. Lett.* **2020**, *15*, 112. [[CrossRef](#)]
306. Wang, L.; Yuan, J.; Zhao, Q.; Wang, Z.; Zhu, Y.; Ma, X.; Cao, C. Supported SnS₂ nanosheet array as binder-free anode for sodium ion batteries. *Electrochim. Acta* **2019**, *308*, 174–184. [[CrossRef](#)]
307. Checko, S.; Ju, Z.; Zhang, B.; Zheng, T.; Takeuchi, E.S.; Marschilok, A.C.; Takeuchi, K.J.; Yu, G. Fast-Charging, Binder-Free Lithium Battery Cathodes Enabled via Multidimensional Conductive Networks. *Nano Lett.* **2024**, *24*, 1695–1702. [[CrossRef](#)]

308. Xia, J.; Yuan, Y.; Yan, H.; Liu, J.; Zhang, Y.; Liu, L.; Zhang, S.; Li, W.; Yang, X.; Shu, H.; et al. Electrospun SnSe/C nanofibers as binder-free anode for lithium-ion and sodium-ion batteries. *J. Power Sources* **2020**, *449*, 227559. [[CrossRef](#)]
309. Gao, X.; An, Y.; Zhang, W.; Yu, M.; Ci, L.; Feng, J. Self-supporting soft carbon fibers as binder-free and flexible anodes for high-performance sodium-ion batteries. *Mater. Technol.* **2018**, *33*, 810–814. [[CrossRef](#)]
310. Kim, H.W.; Kim, H.; Byeon, H.; Kim, J.; Yang, J.W.; Kim, Y.; Kim, J.-K. Binder-free organic cathode based on nitroxide radical polymer-functionalized carbon nanotubes and gel polymer electrolyte for high-performance sodium organic polymer batteries. *J. Mater. Chem. A Mater.* **2020**, *8*, 17980–17986. [[CrossRef](#)]
311. Fu, S.; Ni, J.; Xu, Y.; Zhang, Q.; Li, L. Hydrogenation Driven Conductive Na₂Ti₃O₇ Nanoarrays as Robust Binder-Free Anodes for Sodium-Ion Batteries. *Nano Lett.* **2016**, *16*, 4544–4551. [[CrossRef](#)] [[PubMed](#)]
312. Shen, K.; Zhai, S.; Wang, S.; Ru, Q.; Hou, X.; Hui, K.S.; Hui, K.N.; Chen, F. Recent Progress in Binder-Free Electrodes Synthesis for Electrochemical Energy Storage Application. *Batter. Supercaps* **2021**, *4*, 860–880. [[CrossRef](#)]
313. Lithium-ion Battery Binders Market. Available online: <https://www.marketsandmarkets.com/Market-Reports/lithium-ion-battery-binders-market-143858620.html#:~:text=The%20global%20lithium-ion%20battery,cagr%20from%202022%20to%202027> (accessed on 13 July 2024).
314. Battery Binders Market. Available online: <https://www.precendenceresearch.com/battery-binders-market> (accessed on 13 July 2024).
315. Wood, D.L.; Li, J.; Daniel, C. Prospects for reducing the processing cost of lithium ion batteries. *J. Power Sources* **2015**, *275*, 234–242. [[CrossRef](#)]
316. Duffner, F.; Mauler, L.; Wentker, M.; Leker, J.; Winter, M. Large-scale automotive battery cell manufacturing: Analyzing strategic and operational effects on manufacturing costs. *Int. J. Prod. Econ.* **2021**, *232*, 107982. [[CrossRef](#)]

Disclaimer/Publisher's Note: The statements, opinions and data contained in all publications are solely those of the individual author(s) and contributor(s) and not of MDPI and/or the editor(s). MDPI and/or the editor(s) disclaim responsibility for any injury to people or property resulting from any ideas, methods, instructions or products referred to in the content.